WIRELESS ENGINEER

Vol. XXVII DECEMBER 1950 No. 327

Michael Faraday and the Spinning Bar Magnet

PERHAPS we should apologize for raising again the meaningless but time-honoured question as to whether the field of a cylindrical bar magnet rotates with it when it is rotated about its axis, but we understand that experiments have been made within the last few months with the object of obtaining a definite answer to the question. We need hardly say that the supposed conclusions were entirely fallacious, but, as the experiments were based on some carried out by Faraday, we thought it desirable to look up and study carefully Faraday's descriptions of his experiments. They are given in Volume 1 of his "Researches in Electricity," paragraphs 217 to 230. After studying them carefully we can only admire the clarity of most of his descriptions and discussions, and say quite definitely that he is in no way to blame for the mental fog that seems to have enveloped the subject for many years, in spite of many efforts to dispel it.

The experiments are also described in Faraday's diary Vol. 1, pp. 402–404 and 413–414, and are dated December 1831.

It is interesting to note that the primary object of the experiments was to show that when current was produced by a wire cutting the magnetic curves, (that is, the lines of force) it was not necessary for it to "pass into positions of greater or less magnetic force," but that "always intersecting curves of equal magnetic intensity the mere motion was sufficient for the production of current."

"A copper disc was cemented upon the end of a magnet with paper intervening; the magnet and disc were rotated together and collectors attached to the galvanometer, brought into contact with the circumference and the central part of the copper plate. The galvanometer needle moved as in former cases, . . . Hence rotating the magnet causes no difference in the results, for a rotatory and a stationary magnet produce the same results upon the moving copper."

"A copper cylinder closed at one extremity was then put over the magnet, one half of which it enclosed like a cap; it was firmly fixed (to the magnet) and prevented from touching the magnet by interposed paper. The arrangement was then floated in a narrow jar of mercury, so that the lower edge of the copper cylinder touched the fluid metal; one wire of the galvanometer dipped into this mercury, and the other into a little cavity in the centre of the end of the copper cap." As in the case of the disc, the results were the same when the cylinder rotated, whether the magnet rotated or not.

Then follows an important conclusion. "That the metal of the magnet itself might be substituted for the moving cylinder, disc, or wire, seemed an inevitable consequence, and yet one which would exhibit the effects of magneto-electric induction in a striking form." A cylindrical magnet was floated pole upwards in a jar of mercury, the mercury reaching half way up the magnet. One wire dipped into the mercury, and the other into a drop of mercury in a little hole at the centre of the end. "The magnet was then revolved by a piece of string passed round it, and the galvanometer-needle immediately indicated a powerful current of electricity."

" Thus a *singular independence* of the magnetism and the bar in which it resides is rendered evident" (The italics are Faraday's).

This then would have been Faraday's answer to the meaningless question—Does the field revolve with the magnet ? but seeing that the field was everywhere unchanging in strength and direction, it probably never occurred to him that anyone might imagine that the e.m.f. was induced in the stationary galvanometer leads, and he therefore never mentions their length or location.

In paragraph 224 he says that " experiments were then made for the purpose of ascertaining whether any return of the electric current could occur at the central or axial parts." This presumably meant circulation of current within the rotating magnet. He adds, " the belief being that it could not." In his diary this is worded somewhat differently : he says " The intention was to see whether, when the magnet was rotated, the parts at *ii* etc. could produce currents which the copper rod could discharge down the axis, it having the same angular velocity, as the other parts. It was expected not." A hole of $\frac{1}{4}$ inch diameter was drilled axially to near the middle of the magnet, and an insulated copper rod was passed down it to make contact with a little mercury at the bottom of the hole ; the top projected $\frac{1}{4}$ inch beyond the magnet and carried a small cup of mercury for making contact. The top of the magnet also carried a pool of mercury but insulated from the rod. " The wires A and B from the galvanometer were dipped into these two portions of mercury ; any current through them could, therefore, only pass down the magnet towards its equatorial parts and then up the copper rod ; or vice versa." On rotating the magnet the galvanometer current was in the direction one would expect from the rotation of the magnet in the magnetic field, and the current was small, since the potential at the end of the magnet would not differ much from that of the axis. [Fig. 1(a)].

The magnet was then half immersed in a jar of mercury, the wire A remaining in contact with the top of the rod, while the wire B was removed from the end of the pole to the mercury bath, and therefore in close metallic communication with the equatorial parts of the magnet [Fig. 1(b)]. The current was, of course, much stronger. The wire A was then shifted from the rod to the polar mercury cup, so that the copper rod was out of the circuit [Fig. 1 (c)]. Faraday says, " The current was as strong as it was in the last trial and much stronger than at first." From these results he concludes, " Hence, it is evident that there is no discharge of the current at the centre of the magnet, for the current now freely evolved, is up through the magnet, but in the first experiment it was down. In fact, at that time [Fig. 1 (a)] it was only the part of the moving metal equal to a little disc extending from the end of the wire B in the mercury to the wire A that was efficient ; i.e., moving with a different angular velocity to the rest of the circuit." He apparently saw that, apart from any drop due to its resistance, all parts of the central rod were at the same potential, and that the effective generator was the small disc at the pole end. This is emphasized by his conclusion in paragraph 230 : " In the two after experiments, the *lateral* parts of the magnet or of the copper rod are those which move relative to the other parts of the circuit, i.e., the galvanometer wires ; and being more extensive, intersecting more curves [lines of magnetic induction] or moving with more velocity, produce the greater effect. For the discal part, the direction of the induced electric current is the same in all, namely, from the circumference towards the centre." From this wording it appears that he was regarding the path from the B contact to the A contact as made up of two parts, namely, lateral (or longitudinal) and discal (or radial).

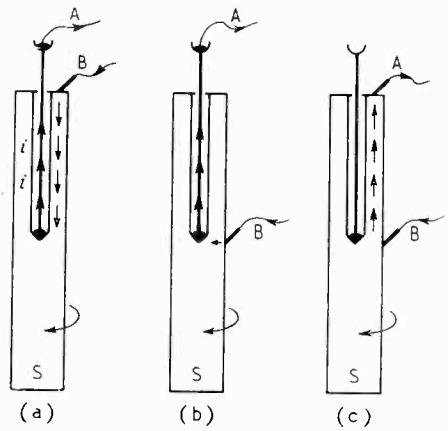

Fig. 1

We should point out that Fig. 1 is not a reproduction but a simplification of Faraday's illustrations.

Light is thrown on the working of his mind by the following interesting quotation from his Diary. " There is evidence of great power in these experiments, for the electricity had only 2, 3 or 4 inches of thick magnet to go through, and yet rather went through 27 or 30 feet of thin copper wire."

The action can, perhaps, be made clearer by considering Fig. 2. All points on the axis are obviously at the same potential, since on no theory does this cut any flux. The equatorial

disc cuts the whole flux of the magnet ; as one approaches the poles the cross-sectional discs cut less and less flux, and the radial e.m.f. induced will vary somewhat as indicated by the curve with base PQ. If the axis is earthed, and the polarity and rotation are as shown, all the potentials and surfaces charges will be positive. Charges will be so distributed throughout the material that the resultant electric force within it is everywhere zero. There will be an electric field between all parts of the magnet surface and the negative charge induced on the earthed surroundings. If, however, the magnet is insulated from earth as it is brought up to speed, the axis and ends assume a negative potential. The potential curve of Fig. 2 retains its shape but, instead of the base PQ being at zero potential, a line such as MN must now represent zero potential, those parts of the curve to the right of it being positive and those to the left negative. Hence the equatorial parts of the surface are positively charged and the end parts negatively charged to an equal amount, so that the mean density of the surface charge is zero. If one were to earth a brush rubbing on the equator, the axis would become more negative still, and the whole surface would be charged negatively to various densities. The line SRT would then represent zero potential.

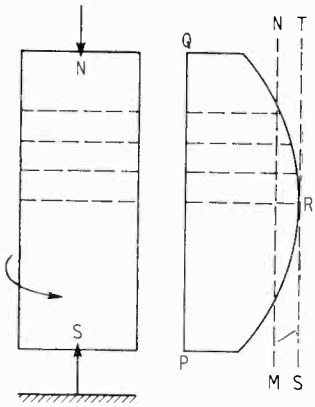

Fig. 2

The rotating bar magnet is a simple form of homopolar generator in which the axis is one terminal and the equator the other. In Fig. 1 we adopted the polarity and direction of rotation employed by Faraday, with which the axis is the positive terminal; in Fig. 2 the rotation is reversed so as to make the equator the positive terminal. The e.m.f. is the same along any path from the axis to the equator. The conditions would be exactly the same if the magnet were replaced by a similar brass cylinder rotating in a current-carrying solenoid producing an equivalent field. In each case a conducting cylinder is rotating in an unchanging magnetic field, and although the question of the rotation or non-rotation of the field has been cropping up for over a century it is surely meaningless.

G. W. O. H.

FERROMAGNETIC MATERIALS AND FERRITES*

Properties and Applications

By M. J. O. Strutt

(Electrotechnical Institute of the Swiss Federal Institute of Technology, Zürich)

Introduction

IN the applications of ferromagnetic materials to communication circuits the reduction of eddy-current losses is always important. These losses, at a given frequency, may be decreased by a reduction of linear dimensions and of the specific conductivity. This latter quantity however, lies within relatively narrow limits in metallic ferromagnetic materials and, as a result, the properties of non-metallic materials were considered as early as forty years ago. However, no really useful materials of this type (mostly iron oxides) have been produced until a few years ago and it is only quite recently that such materials have become available commercially. Thus, a brief consideration of the main points governing their properties and applications seems timely.

*Condensation of three lectures given by the author at London University on February 17th, 21st and 24th, 1949 by invitation.

MS accepted by the Editor, February 1950

Losses in Ferromagnetic Materials

In this discussion, rational units will be mainly used for the electromagnetic and other quantities: V, A, cm, sec. Magnetic field strength H is expressed in A/cm, one of these units being 1.257 oersted. Magnetic induction B is expressed in volt-sec/cm^2, one of these units being equal to 10^8 gauss. Magnetic permeability μ is equal to $\mu_o \mu_r$, where $\mu_o = 4\pi . 10^{-9}$ henry/cm and $\mu_r = 1$ in the case of vacuum.

If we consider thin plates of magnetic material of thickness $2a$ of conductivity γ (mho/cm) placed in a homogeneous alternating magnetic field parallel to its surfaces, we obtain the following expression for the power loss (watts) in a volume V at an angular frequency ω:

$$P_w = \frac{\gamma}{24}\omega^2 4a^2 B^2_{max} V F(2\beta a). \quad .. \quad (1)$$

In this formula B_{max} is the mean value of the amplitude of magnetic induction over the cross-section of the plates under consideration and

$$\beta^2 = \frac{1}{2}\mu_0 \mu_r \gamma\omega \quad .. \quad .. \quad .. \quad .. \quad (2)$$

μ_r being the effective relative permeability of the material at the given B_{max}. The function F

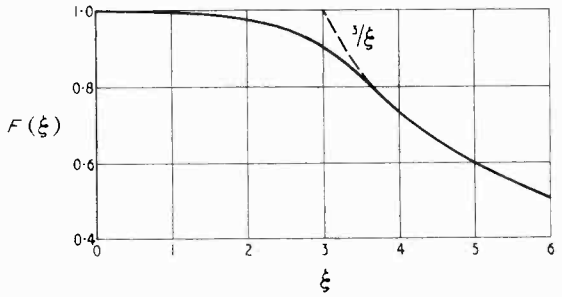

Fig. 1. *Graph of function F of Equ. (1). In the figure the argument of F is denoted by* $\xi = 2\beta a$.

of $2\beta a = \xi$ is shown in Fig. 1. It is seen that F is nearly unity for $\beta a \ll 1$ and is equal to $3/(2\beta a)$ for $\beta a \gg 1$. This implies that a reduction of eddy-current losses is obtained in every case by a reduction of linear dimensions (thickness a) and by a reduction of conductivity γ. These implications are also valid when different shapes of magnetic materials are placed in a homogeneous field; e.g., spheres, cylinders, ellipsoids, etc.

In the applications of ferromagnetic materials in communication circuits, the values of H and B are often so small that Lord Rayleigh's empirical results, obtained half a century ago, may be applied as to the relation between H and B. These results are summarized in Fig. 2, the corresponding expressions being:

if B is increased from $-B_1$ to B_1:

$$B = (\mu_a + \alpha H_1) H - \frac{\alpha}{2}(H_1^2 - H^2)$$

if B is decreased from B_1 to $-B_1$:

$$B = (\mu_a + \alpha H_1) H + \frac{\alpha}{2}(H_1^2 - H^2).$$

Here H_1 corresponds to B_1 and H to B.

We may now assume a cosine function for the dependence of H on time: $H = H_1 \cos \omega t$ and obtain by application of the above expressions, using Fourier's expansion:

$$B = (\mu_a + \alpha H_1) H_1 \cos \omega t + \frac{4}{\pi}\alpha H_1^2\left(\frac{\sin \omega t}{3} - \frac{\sin 3\omega t}{15} - \frac{\sin 5\omega t}{105} \ldots\right). \quad (3)$$

If a coil is properly arranged round the ferromagnetic core, a coefficient of self-inductance L arises at its terminals, expressed by:

$$L = L_0\left(1 + \frac{\alpha H_1}{\mu_a}\right), \quad .. \quad .. \quad .. \quad (4)$$

where L_0 is the value of L at very small values of H_1 such that the second term in brackets is insignificant compared with unity. The first term in brackets of Equ. (3) is a quarter period out of phase with the current in the coil. This obviously corresponds to an additional effective resistance R_h due to the hysteresis loop of Fig. 2:

$$\frac{R_h}{\omega L} = \frac{4}{3\pi}\frac{\alpha H_1}{\mu_a + \alpha H_1} = h_0 H_1 \approx \frac{4\alpha}{3\pi\mu_a} H_1 \quad .. \quad (5)$$

The approximation in the latter part of this equation is tolerable if $\alpha H_1 \ll \mu_a$. The symbol h_0 obviously has the dimension cm/A and is a measure of the loss by hysteresis.

We may express the eddy-current loss by a corresponding resistance R_e. If $\beta a \ll 1$ in Equ. (1), we obtain:

$$\frac{R_e}{\omega L} = \frac{1}{3}a^2\mu_0\mu_r\gamma\omega = \frac{\omega}{\omega_0}. \quad .. \quad .. \quad (6)$$

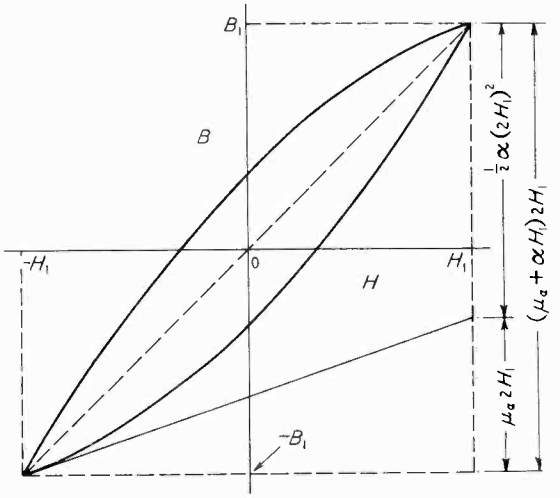

Fig. 2. *Summary of Lord Rayleigh's empirical relations between magnetic induction B and magnetic-field strength H. The hysteresis loop is for H up to about 0.01 A/cm (taken from Ref. 1).*

Here, obviously, ω_0 denotes an angular frequency fixed by the properties of the core:

$$\omega_0 = \frac{3}{a^2\mu_0\mu_r\gamma} \quad .. \quad .. \quad .. \quad .. \quad (7)$$

and the condition $\beta a \ll 1$ is equivalent to $\omega \ll \omega_0$.

This condition is satisfied if the individual parts of the core are of sufficiently small linear dimensions (e.g., thickness a).

Besides the losses by hysteresis and eddy currents, H. Jordan has shown by exact measurements in 1924 the existence of further losses, often indicated as 'residual losses'. These are in urgent need of further experimental and theoretical investigation. The equivalent resistance R_f of these losses may tentatively be expressed by :

$$\frac{R_f}{\omega L} = \epsilon \quad .. \quad .. \quad .. \quad .. \quad .. \quad (8)$$

where ϵ is little dependent on frequency up to, say, 10 kc/s with most materials.

The total equivalent resistance due to core losses is hence[1] :

$$\frac{R_t}{\omega L} = \frac{R_e + R_h + R_f}{\omega L} = \frac{\omega}{\omega_0} + h_0 H_1 + \epsilon \quad (9)$$

Optimal Conditions for Cored Inductances

In many applications of these inductances the quality figure Q should attain a high value. As far as the core losses are concerned, the corresponding quality figure is given by the reciprocal value of the expression (9). A small volume of the inductance in question is obtained by a high value of μ_r. Hence, if high-quality inductances of small volume are desired, the expression $Q\mu_r$ should be considered and should be given as high a value as possible.

There is still another reason for the consideration of the product $Q\mu_r$. If, in a core of completely closed magnetic path, a non-magnetic gap is introduced, the effective value of μ_r decreases to μ_r'. On the other hand the effective value of Q increases to a value Q'. If the original value Q and μ_r satisfy the conditions $Q \gg 1$ and $\mu_r \gg 1$, we have $Q\mu_r = Q'\mu_r'$ as long as $\mu_r' \gg 1$. The introduction of a gap thus gives us a means of obtaining inductances of increased quality Q'.

According to Equ. (9) we may write :

$$\frac{1}{Q\mu_r} = \frac{\omega}{\mu_r \omega_0} + \frac{h_0}{\mu_r} H_1 + \frac{\epsilon}{\mu_r} . \quad .. \quad .. \quad (10)$$

From Equ. (7) we infer that the first term on the right of Equ. (10) is approximately independent of μ_r. As to the second term, the following reasoning may be applied. The value of H_1 is proportional to NI, where N is the number of turns of the inductance in question and I is the effective value of the a.c. through the coil. Furthermore, the coefficient L of self-inductance is proportional to $\mu_r N^2$ and hence H_1 becomes proportional to $I\sqrt{L/\mu_r}$. In many applications of inductances in communication circuits I and L have fixed values. Then obviously, the second term of Equ. (10) becomes proportional to :

$$\frac{R_h}{\mu_r \omega L} \approx \frac{h_0}{\mu_r \sqrt{\mu_r}} . \quad .. \quad .. \quad .. \quad (11)$$

Summarizing, we see that the first term on the right of Equ. (10) is independent of μ_r while the second and the third terms both decrease if μ_r is increased. By using materials of higher μ_r we would hence expect the product $Q\mu_r$ to increase if h_0 and ω do not also increase too much and this increase of $Q\mu_r$ would in itself be desirable in many cases.

However, there is still the distortion caused by hysteresis. This may be inferred from Equ. (3). Considering, in particular, the third harmonic of the alternating voltage at the coil's terminals (due to the core), we obtain for the ratio of the effective third harmonic to fundamental voltage :

$$\frac{V_3}{V_1} = \frac{3}{5} \frac{4\alpha H_1}{3\pi(\mu_a + \alpha H_1)} = \frac{3}{5} \frac{R_h}{\omega L} . \quad .. \quad .. \quad (12)$$

By the application of Equ. (11) it is seen that V_3/V_1 is proportional to $h_0/\sqrt{\mu_r}$. In the known cases of materials with increased values of μ_r, the quantity h_0 also increases and the latter increase is faster than that of $\sqrt{\mu_r}$. Hence, an increase of μ_r would lead to increased distortion. We must conclude that the useful increase of

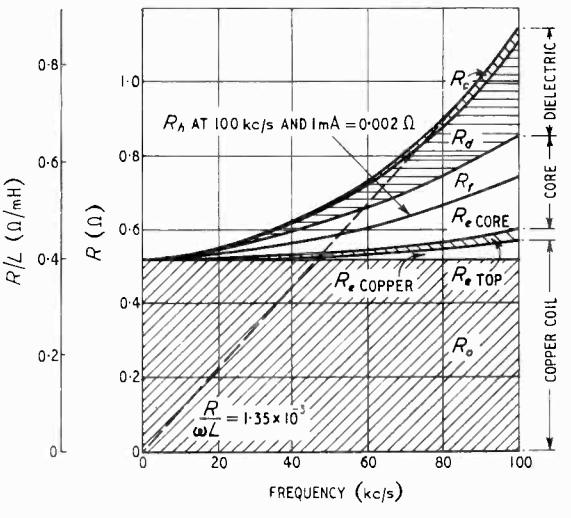

Fig. 3. *Characteristics of inductance with core of carbonyl iron powder embedded in a dielectric binder. The constituent parts of R are : d.c. resistance of coil R_o, additional eddy-current resistance of coil winding R_c, resistance R_{etop} equivalent to eddy-current losses in top and bottom of screening can, R_e equivalent to eddy-current losses of the core, R_h equivalent to hysteresis losses of the core (almost negligible), R_f equivalent to residual losses of the core, R_d equivalent to dielectric losses of insulation, R_c equivalent to dielectric losses of the core (Ref. 4).*

μ_r in magnetic materials is strictly limited by the ensuing distortion in communication circuits.

If the effective value of μ_r is decreased by the application of non-magnetic gaps in the magnetic circuit, the value of h_0 is decreased to h_0' and we have approximately:

$$\frac{h_0'/\sqrt{\mu_r'}}{h_0/\sqrt{\mu_r}} = \left(\frac{\mu_r'}{\mu_r}\right)^{3/2} \quad \ldots \quad \ldots \quad \ldots \quad (13)$$

Hence, the distortion V_3/V_1 is notably decreased by this procedure. At the same time Q is increased and the overall volume of the inductance is also increased.

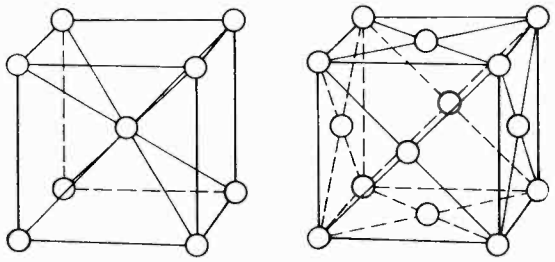

Fig. 4. *Pictures of cubic lattices, body-centred on the left and face-centred on the right.*

Before useful ferrite materials were available the requirements of communication circuits were covered by ferromagnetic materials of two types: granulated iron powders embedded in some suitable dielectric and sheets of suitable alloys[1, 3, 4]. As an example of the first type, the characteristics of an inductance with a ferromagnetic core are summarized in Fig. 3. It is seen that in this case, in which carbonyl iron granules of about 5 microns diameter embedded in a solid dielectric were used as a core, the contribution of hysteresis (R_h) to the overall losses is negligible. The carbonyl iron itself has a permeability μ_r of about 250 but as used in this core, the effective permeability μ_r' is about 15. The optimal value of $1/Q$ occurs at about 80 kc/s and amounts to 1.3×10^{-3}. The value of $h_0'/\sqrt{\mu_r'}$ for this inductance is slightly below 0.05, which complies with international agreements on this figure in communication circuits. Besides this iron-powder material, several types of sheet materials, alloys such as iron-nickel-copper (isoperm), were developed before the war. These could also meet the requirements as to $h_0/\sqrt{\mu_r}$ and Q, and below about 5 kc/s even surpassed the powder cores. Above 5 kc/s, however, powder cores are superior notably due to their smaller eddy losses[1, 3, 4, 5].

Physics of Ferromagnetism

In order to deal with the recent developments of ferrites for inductance cores, a few fundamental ideas about the present theory of ferromagnetism must be reviewed. We shall assume that the ions in a ferromagnetic material constitute a cubic lattice, which may be body centered or face centered (Fig. 4). The electrons, which are more or less mobile in this lattice, behave as tiny magnets owing to their mechanical spin. The ratio of the magnetic moment to the mechanical momentum of any top is, according to P. Blackett, a constant, called gyromagnetic ratio g. There is interaction between the spinning electrons and the ionic lattice, leading to an interaction energy E_i (joule/cm^3). This interaction gives rise to certain domains, named after P. Weiss, in which the magnetization has a preferred direction[1, 9]. The energy, required to turn one cm^3 of the substance in such a domain from the direction of minimum to that of maximum energy is called the 'anisotropy energy' E_a (joule/cm^3). The value of E_a is depicted in Fig. 5 for a cubic crystal, the edges of which are parallel to x, y and z. The directions of minimum E_a are parallel to the edges of the crystal. If a stress anisotropy exists, the values of E_a are altered, as shown in Fig. 5. The minimum stress σ occurring in any

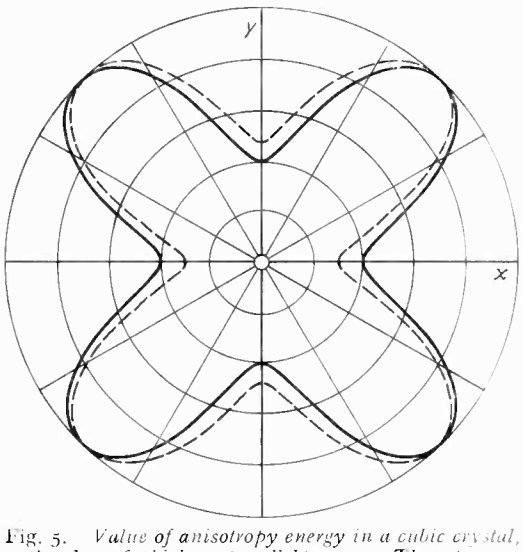

Fig. 5. *Value of anisotropy energy in a cubic crystal, the edges of which are parallel to x, y, z. The representation makes use of a polar diagram. The full curve corresponds to the case without stress, the broken curve to the case of a relatively small superimposed stress (taken from Ref. 1).*

material is such that the specific extension is of the order of magnitude of the magnetostriction value λ. Hence $\sigma_{min} \approx \lambda E$, where E is Young's modulus. For iron this yields $\sigma_{min} \approx 100$ kg/cm^2.

From this we see that E_a may, in general, be attributed to two different causes, the crystal

anisotropy energy E_c (joule/cm^3) and the stress anisotropy energy $\sigma\lambda$ (joule/cm^3). In a given material, preponderance of E_c as well as of $\sigma\lambda$ may occur[1].

Ferromagnetic theory, though still rudimentary, indicates that the initial permeability μ_r is high, if E_c and $\sigma\lambda$ are small. Furthermore, the relative width of the hysteresis loop of Fig. 2 is small, if E_c and $\sigma\lambda$ are small. Thus, we must search for materials in which E_c and $\sigma\lambda$ are small simultaneously[1].

Some binary and ternary alloys are known, in which these conditions prevail at room temperature[7] (e.g., Sendust).

Composition of Useful Ferrites

It has been known for a very long time that the natural cubic ferrous ferrite $FeOFe_2O_3$ (magnetite) has ferromagnetic properties. Its behaviour as to maximum magnetization, anisotropy energy E_a, magnetostriction and permeability is comparable to that of nickel. Other ferrites may be obtained by substituting another bivalent metal of approximately equal ionic volume for the iron in the FeO component of the above material, the structure of which is of spinell type. Thus we obtain the following examples of cubic ferrites : $MgOFe_2O_3$, $NiOFe_2O_3$, $CoOFe_2O_3$, $ZnOFe_2O_3$. The last substance is nonmagnetic at room temperature, the others are ferromagnetic[7].

At the Curie temperature a ferromagnetic substance becomes nonmagnetic and remains so at higher temperatures. The above property of zinc ferrite points to its Curie temperature being below room temperature, while the Curie temperatures of the other ferrites are higher. By suitably mixing zinc ferrite with other ferrites we may obtain Curie temperatures between room temperature and the Curie temperatures of the other ferrites. The crystal anisotropy energy E_c becomes very small if the Curie temperature is approached, long before the substance becomes nonmagnetic. The value of λ, however, remains different from zero almost up to the Curie temperature. Hence we may conclude that E_c may be made sufficiently small at room temperature by the choice of a Curie temperature (obtained by a suitable mixture as observed above) not too far above room temperature. We must, however, apply a different procedure to decrease λ at room temperature. Now experimental evidence points to λ being of negative sign for all single ferrites (see the above examples) except $FeOFe_2O_3$, in which λ is of positive sign at room temperature. By the formation of suitable mixed crystals of the latter ferrite with any of the former, very small values of λ may be obtained at room temperature. Combining this evidence with the above on the addition of zinc ferrite it is seen that low values of E_c as well as of λ simultaneously may be obtained at room temperature by a suitable choice of ferrite components. The application of this basic idea has led to useful ferrites, having high initial permeability as well as low hysteresis losses[7]. Althouth the application of ferrites was patented more than 40 years ago with a view to a decrease of the eddy-current losses in cores owing to the low conductivity of these materials, their low permeability and high hysteresis losses prevented them from being really useful up to quite recently. Due to the above basic ideas, however, these difficulties in the application of ferrites have now been overcome.

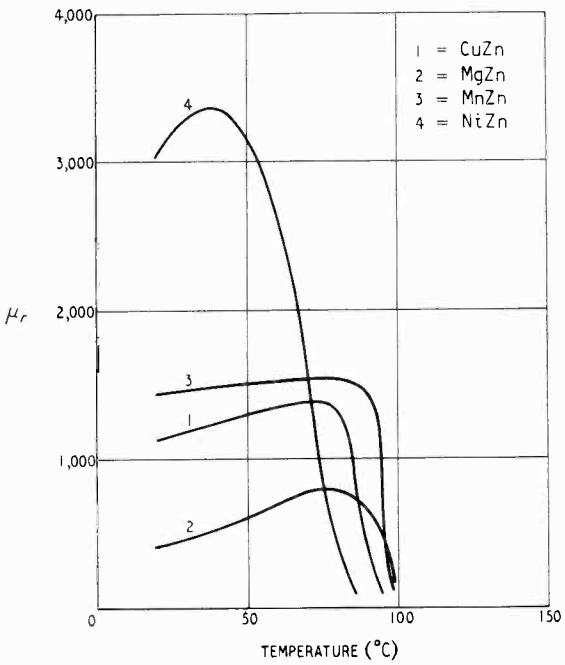

Fig. 6. *Dependence of initial relative permeability μ_r of ferrites types 1 to 4 (see Table 1) on temperature (taken from Ref. 7).*

It is obvious that a very careful selection of components and preparation of the products are required in order to achieve the indicated aims[7]. A cubic structure of the final ferrite is conducive to avoidance of stresses arising during the cooling down after sintering the components at temperatures of about 1200°C. This is due to the equal shrinking of cubic crystals in all directions. Polycrystalline aggregates of non-cubic structure tend to develop internal stresses upon cooling on account of anisotropy of shrinking. Such stresses may cause low permeability and high hysteresis losses.

In the preparation of the ferrites the proper oxides are pulverized and mixed thoroughly in the desired proportions. Thereupon a binder is added and the resulting plastic material is moulded; e.g., to rods and tubes. Another procedure is to put the dry powder into matrices and apply moulding under high pressure. Then a sintering process is applied to the moulded mass. The heating and cooling must be carried out in carefully determined cycles using special electric furnaces. In order to avoid chemical reactions of the sintering mass with the surrounding atmosphere, a special nitrogen atmosphere is in some cases provided during the sintering process. The sintered products, similar to certain ceramic materials, are of considerable hardness and may only be ground if further treatment is required. The linear tolerances of the sintered products are about 2 per cent. If smaller values are necessary, grinding must be applied[7].

Four examples of useful ferrites are given in Table 1 together with some pertinent data. Each product is a mixture of two ferrites; e.g., the first one of $CuOFe_2O_3$ and $ZnOFe_2O_3$, the proportion of Cu to Zn to Fe_2O_3 molecules being 20 : 30 : 50; i.e., exactly equimolecular. This latter feature is also true for the three other examples[7].

The long term stability of the ferrites is important for some applications. During the first months after production the initial permeability μ_i decreases a little, usually about 1 or 2 per cent. Upon magnetization in a strong field the variation of μ_i is of the same order of magnitude. The value of μ_i is dependent on temperature, as shown in Fig. 6. Between 10°C and 40°C its variation is in some cases about 0.2 per cent per degree. By the application of non-magnetic gaps the effective variations may of course be made smaller than the above figures.

Application of Ferrites

The eddy-current losses in ferrites, owing to their relatively low conductivity, are almost negligible in most practical applications up to about 100 kc/s. This may be seen from Equ. (1). In iron the conductivity γ is of the order of magnitude 10^5 mho/cm, while the highest value with the above ferrites is 0.02. Thus the losses, at equal values of a, ω, F and B_{max} would be about 10^7 times smaller with the ferrites. Conversely, for equal losses ferrite cores may be at least some thousand times thicker than comparable iron ones at the same frequency and the ratio holds for the frequency if the cores are the same thickness. Hysteresis losses in

Fig. 7 (below). *Three comparable inductances containing cores of sheet alloy, of iron powder embedded in a a dielectric and of ferrite (on the right). The inductances being equal, the quality Q of the two coils on the left is about 220 at 60 kc/s, whereas the quality Q of the ferrite coil on the right at this frequency is 550.*

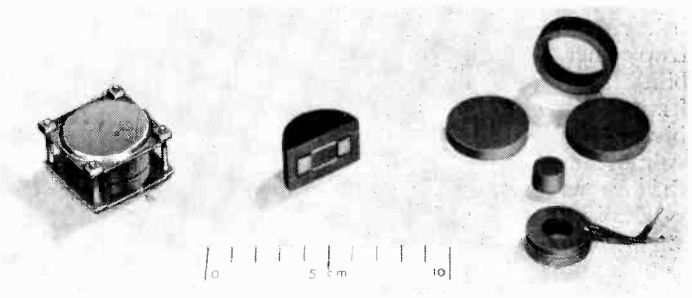

Fig. 8 (right). *Construction of ferrite-cored inductance of Fig. 7, the coil being wholly enclosed by ferrite material.*

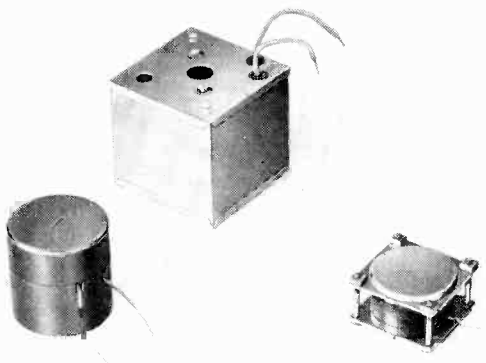

TABLE 1

Type	Proportion	Curie Temp. (°C)	Conductivity at 20° (mho/cm)	Optimal μ_i obtained
1	$Cu/Zn/Fe_2O_3$ = 20/30/50	90	5×10^{-5}	1500
2	$Mg/Zn/Fe_2O_3$ = 25/25/50	100	2×10^{-6}	700
3	$Mn/Zn/Fe_2O_3$ = 25/25/50	100	2×10^{-2}	2000
4	$Ni/Zn/Fe_2O_3$ = 15/35/50	75	2×10^{-4}	4000

ferrites are also relatively small. The figure to be considered in most communication circuits is $h_0/\sqrt{\mu_r}$. This is given in Table 2 for some materials[7]. From this Table it is seen that the alloy called isoperm (about 50 per cent iron, 40 per cent nickel and 10 per cent copper) is superior as to relative distortion in communication circuits. Second is the ferrite type 3. Now the alloy must be applied in sheets in order to avoid eddy losses and hence is less suitable

TABLE 2

Material	μ_r	$h_0/\sqrt{\mu_r}$
Isoperm	85	3×10^{-4}
Permalloy	9000	3×10^{-2}
Sendust	55000	6×10^{-2}
Carbonyl iron	250	3×10^{-2}
Ferrite type 3	1000	8×10^{-3}

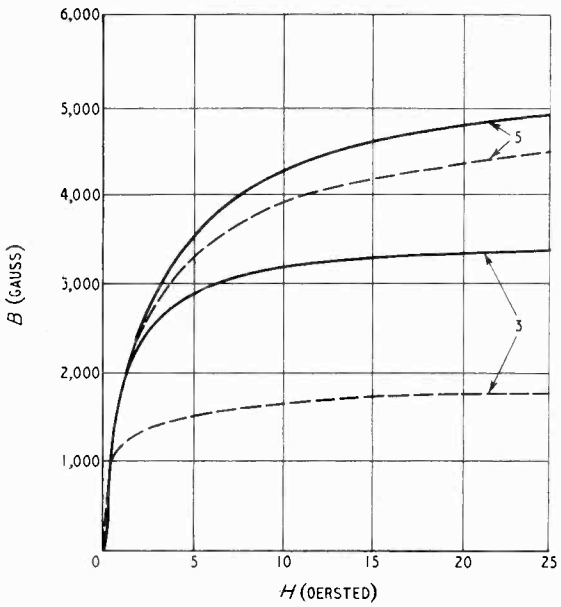

Fig. 9. *Magnetic induction as dependent on magnetic-field strength. The curves are for two types of ferrites, one of which is type 3 of Table 1. The solid line curves are for a temperature of 20° C and the dash-line is for 80°C.*

above, say, 5 kc/s. From this frequency onwards the ferrite material is preferable. By inserting gaps, the above values of μ_r and of $h_0/\sqrt{\mu_r}$ may be reduced according to Equ. (13).

Because of their high initial permeability μ_r some ferrites provide very effective screening of magnetic fields inside suitably-shaped cored inductances from the external space. The usual screening cans are hence far less affected by the internal alternating fields and thus the eddy-current losses in the can may be effectively reduced. The can dimensions may also be reduced and hence the overall dimensions of the inductances may be decreased. An example of a ferrite-cored inductance is shown in Fig. 7 compared with two other types, all being

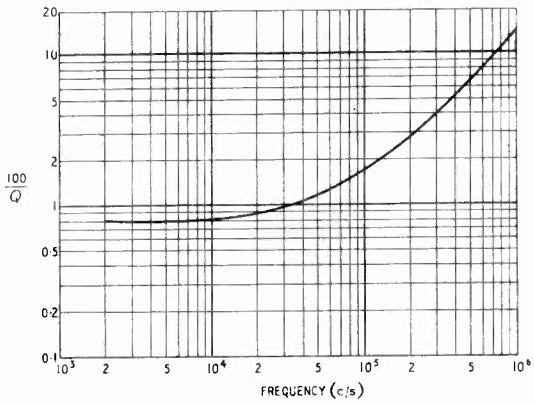

Fig. 10. *Plot of 100/Q against frequency for an inductance with a core of ferrite type 3 of Table 1 (taken from Ref. 8).*

suitable for use at 60 kc/s. The right-hand one has a core of ferrite type 3 and is smaller than the other two. The overall value of Q at 60 kc/s is about 600. The coil is entirely embedded in ferrite as shown in Fig. 8 in which the core construction, including two gaps, is seen.

The B–H curves of two ferrites, H being in oersted and B in gauss, are shown in Fig. 9 at the temperatures 20° and 80°C. It is particularly notable that the saturation value of magnetic induction is relatively low with these materials, as compared with sheet materials used in transformers. Owing to these low saturation values the application of ferrites in power-transformers is less desirable, for they would become too bulky.

As eddy-current losses and hysteresis losses are small in suitable ferrite cores, the residual losses corresponding to the third term on the right of Equ. (9) are of particular interest. These losses, together with the eddy-current losses, limit the applications of ferrite cores at high frequencies. This is shown in Fig. 10, picturing the reciprocal quality-figure $1/Q$ as dependent on frequency for a ferrite-cored inductance[8]. It may be shown theoretically that the sharp rise of $1/Q$ is due mainly to a rapid increase of the residual losses at a specific higher frequency which is characteristic to the material in question. The specific frequency at which the sharp rise of residual losses occurs is approximately inversely proportional to the initial

permeability μ_r of the ferrite material in the core. Hence, materials of lower μ_r may in general be used up to higher frequencies. Furthermore the rise is sharper if the material is of more homogeneous structure. The former fact is illustrated by a comparison of Figs. 10

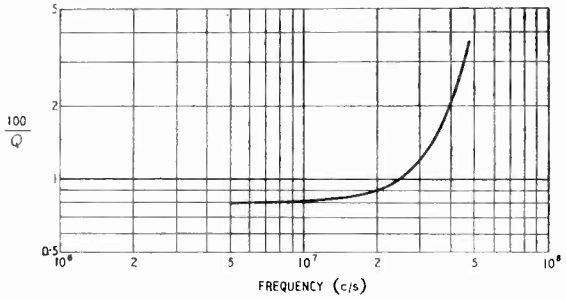

Fig. 11. *Plot of 100/Q against frequency for a core of ferrite type 4 of Table 1. The ratio of initial permeabilities of ferrites types 1 to 4 is about 1000/50 for the ferrites used in the experiments (taken from Ref. 8).*

and 11, as the initial permeabilities of the ferrites used in Fig. 10 and Fig. 11 are about 1 000 and 50 respectively[7, 8].

By their low losses at not too high frequencies ferrite cores are suitable for the construction of transformers if bulk does not constitute a particular consideration. Such almost loss-free transformers, if suitably wound, may offer better approximations to 'ideal' transformers than were hitherto obtainable using other core materials at moderately high frequencies.

Finally, the application of ferrite cores in magnetic amplifiers will be considered briefly. In cores of such amplifiers low losses are essential in view of the auxiliary oscillating flux which is required. In the case of d.c. amplifiers it is useful to apply a relatively high auxiliary frequency in order to reduce the time constant. In the case of a.c. amplifiers this requirement is even more stringent and the metallic ferromagnetic materials are in most cases unsuitable for the construction of such magnetic amplifiers. Here ferrite cores may fill the gap and thus make the construction of efficient a.c. magnetic amplifiers possible[6].

REFERENCES

Only some fundamental papers are listed below. These contain a large number of further references.

[1] Becker, R. and W. Doring, "Ferromagnetismus," Springer, Berlin, 1939.

[2] Becker, J. A., C. B. Green and G. L. Pearson. "Properties and Uses of Thermistors (Thermally Sensitive Resistors)" *Electrical Engineering*, Nov. 1946.

[3] Dahl, O. and J. Pfaffenberger. "Hysteresearme und stabile Werkstoffe fur die Fernmeldetechnik (Isoperme)," *Zeitschrift für technische Physik*, Vol. 15 (1934) pp. 99–106.

[4] Goldschmidt, R. "Die Werkstofforderungen der Fernmeldetechnik unter besonderer Berücksichtigung des Pupinspulenbaues," *Zeitschrift für technische Physik*, No. 15 (1934) p. 95.

[5] Kersten, M. and H. Hesse. "Hysteresearme Massekern-spulen für das Trägerfrequenz-Fernsprechen. *Elektrische Nachrichtentechnik*, Vol. 14 (1937) pp. 66–74.

[6] Landon, V. D. "The Use of Ferrite-cored Coils as Converters. Amplifiers and Oscillators," *R.C.A. Review*, September 1949, pp. 387–396.

[7] Snoek, J. L. "New Developments in Ferromagnetic Materials." Monographs on Research in Holland, Elsevier, Amsterdam 1949.

[8] Snoek, J. L. "Dispersion and Absorption in Magnetic Ferrites at Frequencies above one Mc/s." *Physica*, (The Hague), Vol. 14 (1948) pp. 207–217.

[9] Strutt, M. J. O. and K. S. Knol, "Determination of Magnetic Permeability at 100 Mc/s, etc." *Physica*, (The Hague), Vol. 7 (1940) pp. 635–654.

UNIVERSAL DECIMAL CLASSIFICATION

The Fédération Internationale de Documentation is introducing a new service to U.D.C. users. This is the production of a half-yearly cumulative list of Proposed Extension notes to be known as Extensions. The first will contain all P.E. notes published and approved during the first half of 1950. The annual subscription is £2 10s. and orders may be placed with the Sales Department of British Standards Institution, 24/28, Victoria Street, Westminster, London, S.W.1.

F.B.I. REGISTER

The 1950/51 edition of the F.B.I. Register of British Manufacturers is the only authorized directory of the Federation of British Industries. Over 6,000 firms are included in its 832 pages together with addresses, trade marks, brands and trade names. The book is compiled and classified for quick reference with major instructions and cross references in English, French and Spanish.

Priced at 42s., the book is obtainable from Kelly's Directories, 186, Strand, London, W.C.2 (home) and Iliffe & Sons, Ltd., Dorset House, Stamford Street, London, S.E.1 (overseas).

On account of the recent dispute in the printing trade, the publication of *Wireless Engineer* is still somewhat delayed. This issue, which is dated December, has been expanded to include double the normal number of Abstracts and Reference pages; it includes abstracts which would have normally appeared in the November and December issues.

PULSE GENERATOR OF FIXED REPETITION RATE

With Sine-wave Control

By F. A. Benson, M.Eng., A.M.I.E.E., and R. M. Pearson, B.Eng.

(The University of Sheffield)

SUMMARY.—A simple pulse generator with a fixed repetition rate is described. The negative pulses which it produces have a time of rise of 0.8 microsecond and an amplitude of about 60 volts. The circuit can be built from a few normal laboratory components and requires no rectifier unit for it operates from an alternating voltage of about 200 V r.m.s.

Introduction

THE circuits most commonly used for the production of pulses at a fixed repetition rate work on the principle or clipping an input sine wave and passing the resultant 'square' wave through an RC differentiating circuit from which a succession of positive and negative pulses is obtained. The sequence is illustrated in Fig. 1. As shown in Fig. 2, clipping can conveniently be obtained by using either a pair of biased diodes (a) or a pentode (b) in which grid current removes the top of the positive half cycle and cut-off does the same for the negative half cycle. In both cases the time of rise of the output pulse and its amplitude are dependent on how near the output of the clipping stage approximates to a true square wave.

If the maximum amplitude of the input sine wave is V and that of the clipped wave is h (Fig. 2), then if $V \gg h$

$$\delta t \approx h/\pi V f.$$

where δt is the time taken to rise from $-h$ to $+h$ and f is the frequency.

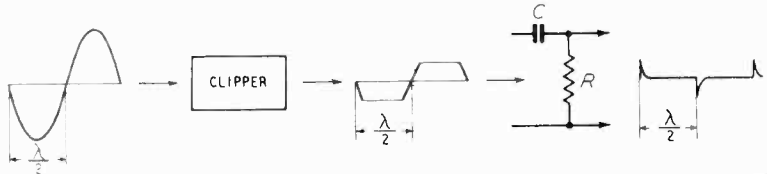

Fig. 1. *A common method of producing pulses from a sine wave is by clipping and differentiating.*

As a typical example assume $V = 250$ V and $h = 2$ V. Then a frequency of 50 c/s gives $\delta t = 50$ μsec and a frequency of 500 c/s gives $\delta t = 5$ μsec.

RC differentiation theory shows that the introduction of a voltage step with a finite time of rise produces a pulse whose rising slope is at

MS accepted by the Editor, February 1950

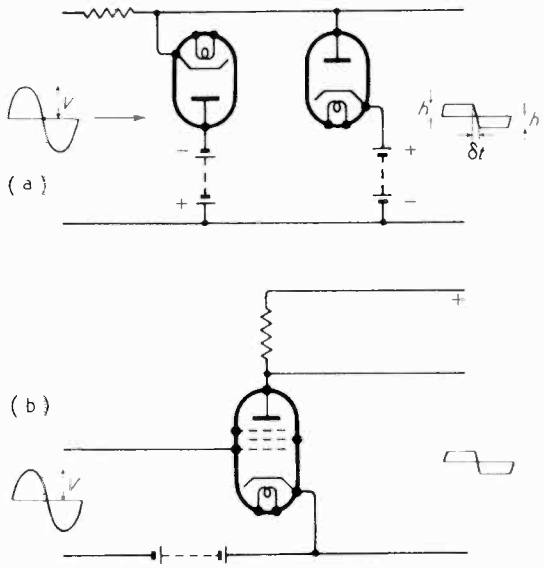

Fig. 2 (above). *Typical clipping circuits are shown; (a) is a pair of biased diodes and (b) a pentode.*

Fig. 3. (below). *Circuit of pulse generator.*

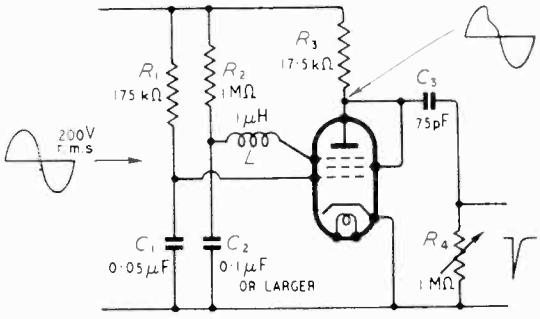

best only equal to the slope of the input. Thus, to obtain a time of rise of less than a microsecond by this method the clipper output must be amplified again and reclipped.

The present article describes an alternative method employing a simple circuit which produces a succession of negative pulses at a repetition rate equal to the frequency of the input sine-wave. The pulses have a time of rise of 0·8 microsecond, an amplitude of about 60 V and an exponential decay which may be controlled by the value of the resistance in an RC differentiating circuit.

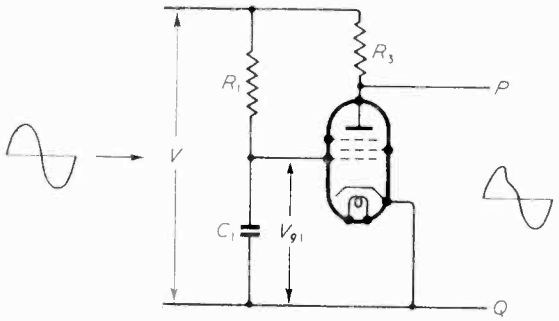

Fig. 4 (above). *Illustrating the action of the control-grid and anode circuits.*

Fig. 5 (below). *Vector diagram of the grid and anode voltages* (a). *The various voltage waveforms* (b). *Typical* I_a-V_g *curves are shown in* (c).

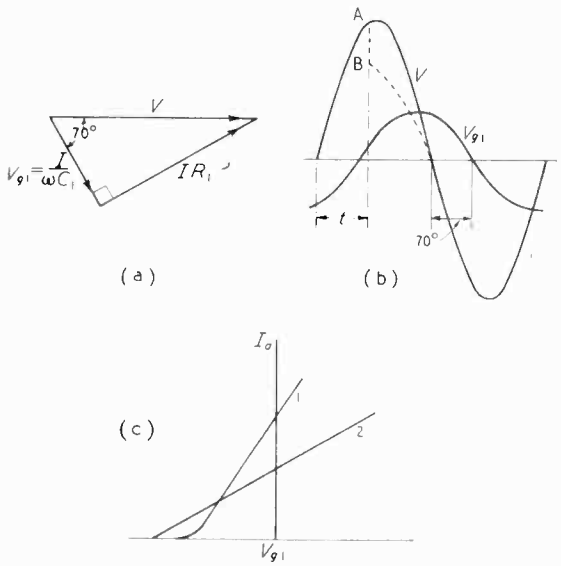

Circuit Arrangement

The circuit is shown in Fig. 3. The valve used is a pentode, the suppressor-grid circuit of which can be made to display negative-resistance characteristics. An alternating voltage is applied between anode and cathode of the valve. Two alternating voltages, both differing in magnitude and phase from the supply voltage, are simultaneously applied to the control and suppressor grids via R_1C_1 and R_2C_2. The action takes place on those half cycles when the anode is positive with respect to the cathode.

Consider first the part played by the control grid and associated circuit. In the simple circuit of Fig. 4 a voltage V is applied between anode and cathode. The magnitude of voltage V_{g1} applied to the control grid and its phase with respect to the anode voltage are given by the vector diagram of Fig. 5 (a). In this case the values of R_1 and C_1 are such that the voltage V_{g1} lags V by 70°. Thus considering the cycle shown in Fig. 5 (b) the valve is cut off until some time t when the grid has become sufficiently positive. At this point there is a sudden increase in anode current and the resulting anode wave-

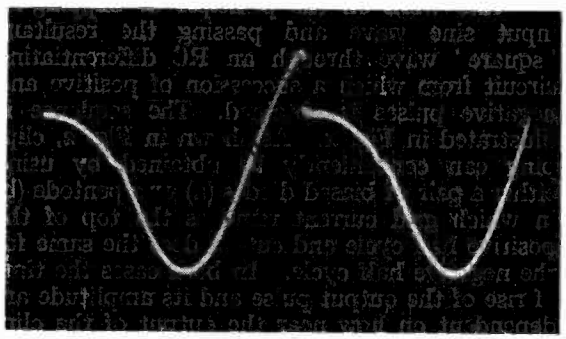

Fig. 6. *Oscillogram of anode voltage with the complete circuit of Fig. 3.*

form in shown dotted. The steepness of the voltage drop A to B depends on the slope of the I_a–V_g characteristics of the valve immediately after cut-off; i.e., a characteristic of the form (1) in Fig. 5 (c) will produce a steeper drop than will one like (2).

If a simple RC differentiating circuit is connected across P and Q of Fig. 4, pulses will be obtained due to the drop in voltage A to B in Fig. 5 (b). These pulses are of some 60 V amplitude but their time of rise is poor, being only about 20 μsec at best.

The effect of additional connections and components will now be considered. The screen grid is strapped to the anode and R_2, C_2 and L (in Fig. 3) are introduced into the suppressor-grid circuit. L, with the valve and stray capacitances to earth, forms a tuned circuit. Conditions are adjusted so that this tuned circuit executes one half cycle of a triggered relaxation oscillation, the net effect of which is to give an extremely rapid fall of suppressor voltage causing

a similar rapid fall of anode voltage within the interval A–B of Fig. 5 (b). This can be seen on the oscillograph trace of anode voltage (Fig. 6). When differentiated by R_4, C_3, pulses with very short time of rise are produced.

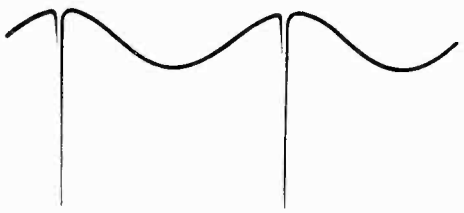

Fig. 7. *Output pulses superimposed on the input sine wave.*

It will be observed that this pulse is superimposed on the supply voltage as illustrated in Fig. 7. The amplitude of the sine-wave in the output, however, can be reduced to a negligible value by the correct setting of R_4.

Explanation of Triggering

A set of suppressor-grid current—grid-voltage characteristics was taken with the screen grid strapped to the anode and an anode load resistance in circuit. Results for three different anode loads are shown in Fig. 8. The characteristics are seen to possess negative-resistance regions. The shape of these regions varies greatly with the anode voltage which, in this circuit, is determined to a large extent by the value of the anode load resistor. The negative-current properties are assumed to be due to secondary emission from the suppressor-grid. If the suppressor is taken far enough positive, the current in all cases rises rapidly into the positive region after a certain point is reached, although this is not shown in all the characteristics.

As stated previously the 1-μH inductor L forms a parallel LC circuit with the valve and stray capacitances.

Consider the suppressor-grid circuit of Fig. 9; $C_2 \gg C_0$, thus as regards any h.f. oscillations or sudden changes the point B is at cathode potential. The parallel circuit LC_0 is across a negative resistance and analysis of this type of circuit results in the differential equation :—

$$p^2 i + (1/\rho C_0 + r/L)\, pi + (r + \rho)\, i/\rho LC_0 = 0$$

where ρ is the value of the negative resistance, r the resistance of the LC_0 circuit, i the current through L and p the operator d/dt.

The solution of this equation is :—

$$i = Ke^{\alpha t} \sin(\beta t + \epsilon)$$

where $\alpha = -(1/\rho C_0 + r/L)/2$

$$\beta = \sqrt{[(r + \rho)/\rho LC_0 - (1/\rho C_0 + r/L)^2 +]}$$

and K and ϵ are constants depending on the initial conditions.

Oscillations result if $1/\rho C_0 + r/L$ is negative. They can be sinusoidal or relaxation oscillations depending on whether β is real or imaginary.

In practice a train of steep-sided relaxation oscillations results and produces the anode waveform shown in Fig. 10. It starts when the LC_0 circuit receives an impulse due to the fast increase of space current in the valve when the control grid voltage emerges from the cut-off region as discussed in connection with Fig. 4. The steep side of the first oscillation cycle occurs

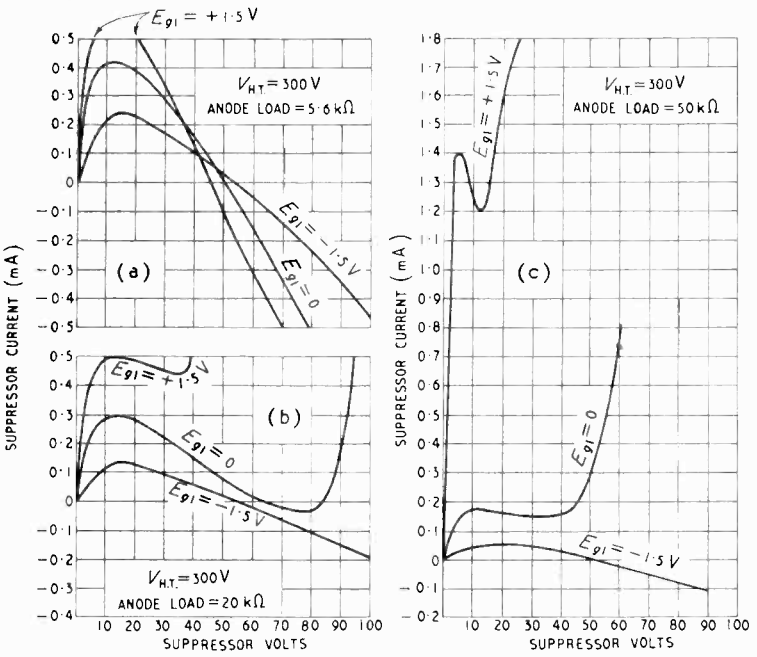

Fig. 8 (left). *Grid-current—grid-voltage curves for the suppressor grid.*

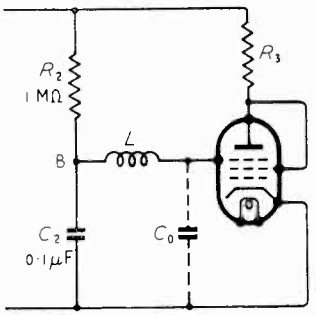

Fig. 9 (above). *Suppressor-grid circuit of the generator.*

in the interval AB of Fig. 5(b). It is required to produce only one pulse per applied a.c. cycle, therefore phase conditions in the practical circuit are adjusted so as to inhibit all but this first half cycle. The angle of lag of the control-grid voltage behind that of the applied a.c. is adjusted so that the fast drop in anode voltage in the interval AB occurs at the instant the suppressor-grid begins to draw heavy positive

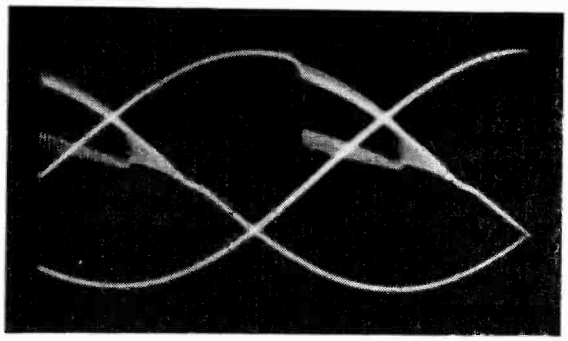

Fig. 10. *Anode-voltage waveform of the generator.*

current (this can be done by viewing the suppressor-grid waveform on an oscilloscope and adjusting R_1). When this occurs the tuned circuit LC_0 is very heavily damped. The output pulse is shown in Fig. 11.

Conclusions

The pulse generator described has the great advantage over the other types mentioned in that the only power supplies required are an a.c. one of about 200-V r.m.s. amplitude, whose frequency is equal to the required pulse repetition rate and one for the heater of the valve. Further, the circuit can be constructed from a few normal laboratory components. Thus, without any necessity for the use of a rectifier unit, and amplifiers, sharp pulses of good amplitude are easily obtained.

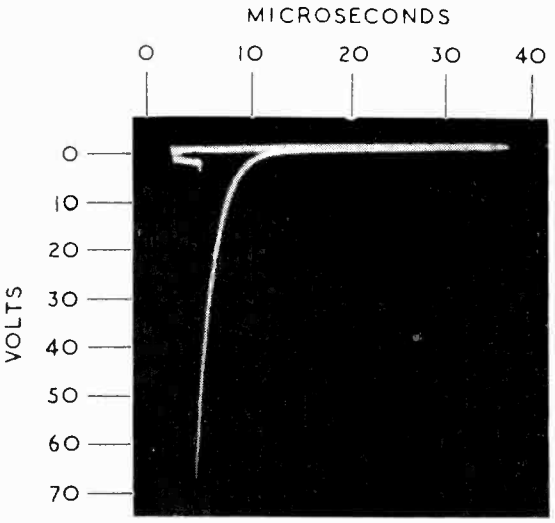

Fig. 11. *Output voltage pulse.*

Acknowledgment

The work recorded in this paper has been carried out in the Department of Electrical Engineering at the University of Sheffield. The authors wish to thank Mr. O. I. Butler, M.Sc., M.I.E.E., for facilities afforded in the laboratories of this Department.

CATHODE-FOLLOWER PERFORMANCE

Pulse and Saw-tooth Conditions

By A. J. Shimmins, B.E.E., B.Com.

(E.M.I. Engineering Development—Advanced Development)

1. Introduction

THE behaviour of cathode-follower circuits, mainly as impedance matching devices, is well known, and a considerable amount of information is available about their operation with sinusoidal signals of relatively small amplitude. It is proposed here to use Laplace-transform methods to find the factors which determine the behaviour of the circuits under pulse conditions. It will be shown that for the general case of a cathode-follower with a capacitive load, the input impedance of the circuit can be quite low to a steep-fronted input pulse in that, even with relatively small input signals, grid current will flow during the rise time of the output pulse. In addition, considerable distortion can occur to the trailing edge of the pulse if the input voltage decreases sufficiently rapidly to cause the valve to be cut off.

The distortion of voltages of saw-tooth waveforms, which are used for radar time bases, is also analysed.

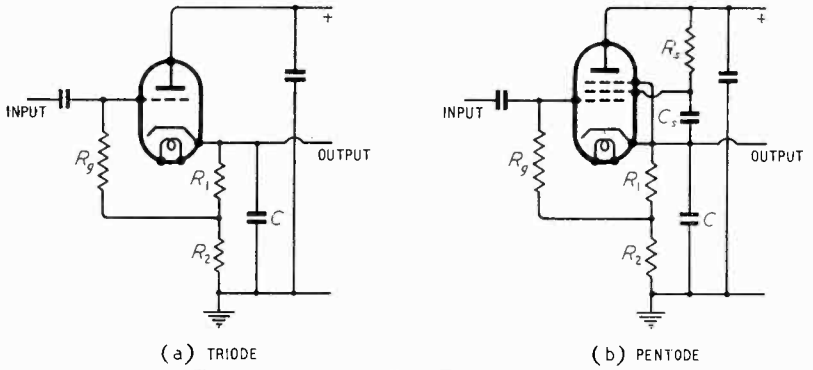

Fig. 1. *Typical cathode-follower circuits.*

2. Pulse Response

Consider a typical cathode-follower circuit with capacitive loading as shown in Fig. 1.

Assuming that the equivalent circuit of the valve is applicable (i.e., the valve characteristics are straight and parallel and equally spaced), the increment of current through R_1 and R_2 above the quiescent value is given by :—

$$r_a CR\frac{di_R}{dt} + i_R\{(\mu+1)R+r_a\} = \mu e_{in} \qquad (1)$$

MS accepted by the Editor, January 1950

where

r_a = anode resistance of valve
C = shunt capacitance across load.
R = total cathode resistance $= R_1 + R_2$
μ = amplification factor
e_{in} = the applied input voltage
i_R = current increment in $R_1 + R_2$

The solution of this equation for an applied voltage of the form $e_{in} = E(1 - e^{-t/T})$ is given by :— (See Appendix 1)

$$i_R = \frac{AE}{R}\left(1 - \frac{Te^{-t/T} - T_0 e^{-t/T_0}}{T - T_0}\right)$$

Therefore $$e_{out} = AE\left(1 - \frac{Te^{-t/T} - T_0 e^{-t/T_0}}{T - T_0}\right) \qquad (2)$$

where

T = time constant of the input voltage
$T_0 = R_0 C$ = time constant of output impedance and load capacitance. R_0, the output impedance, is equal to $\dfrac{Rr_a}{(\mu+1)R + r_a}$
A = gain of cathode-follower.
$= \dfrac{\mu R}{(\mu + 1)R + r_a}$

Equation (2) is perfectly general and gives the change in cathode voltage above or below the quiescent value for a specified change in input voltage of known time constant T. When t is large so that the exponential components have decayed, the output voltage tends to AE. (E is the maximum value of the input voltage.)

3. Response to Positive Step

In this case E is positive and corresponds to the leading edge of a positive pulse or the trailing edge of a negative pulse. For the particular case of a step function input, $T = 0$ and

$$e_{out} = AE\,(1 - e^{-t/T_0}) \qquad (3)$$

and the output is an exponential rise of time constant equal to $R_0 C$.

The output responses for two input voltages of different rise times are given in Fig. 2(a) and (b). It should be noted that if T is greater than

about 5 times T_0, the output voltage follows the input voltage fairly closely.

From Fig. 2 it can be seen that if T is of the same order as T_0 the cathode potential cannot follow the grid voltage immediately. Consequently, the grid becomes positive and grid current flows, until the cathode voltage builds up and exceeds the grid voltage.

For a large step function input, grid current flows (with consequent low input impedance) for a time approximately 3 times the time constant T_0 of the output circuit.

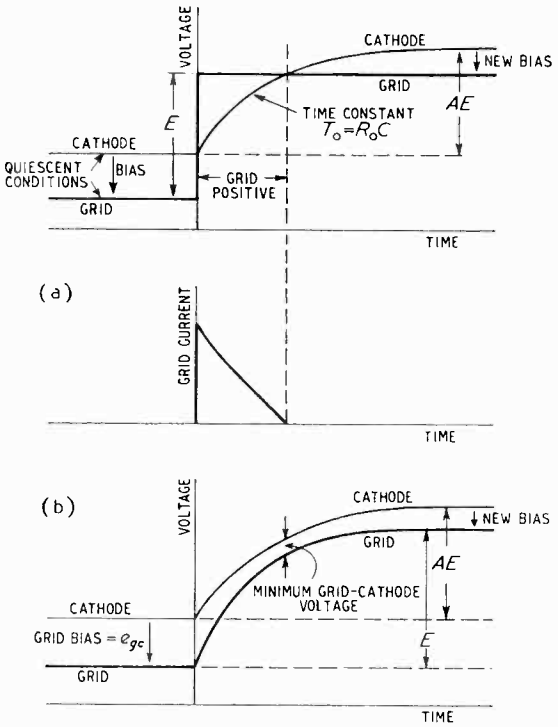

Fig. 2. *Response to a step function (a) and to an exponential rise at the grid (b).*

It can be shown that the necessary condition for grid current to flow is given by :—

$$E(1-A) \geqslant e_{gc} + E\left(e^{-t/T} - A\frac{e^{-t/T} - T_0/Te^{-t/T_0}}{1 - T_0/T}\right) \quad \ldots \quad (4)$$

where e_{gc} is the grid-cathode voltage before application of the input pulse, and the other symbols have the same meaning as in equation (2), and that the most likely time for grid current to flow, or the time when the grid current is a maximum, is given by :—

$$t = \frac{T_0 T \log_e (T_0/TA - 1/A + 1)}{T_0 - T} \text{ sec} \quad (5)$$

after the application of the input pulse. If $T = 0$ (a step function) the maximum current is at the beginning of the pulse.

4. Response to Negative Step

If a negative step, corresponding to the trailing edge of a positive pulse or the leading edge of a negative pulse, is applied to the grid of a cathode-follower, equation (2) still holds, but in this case E is negative. The changes in grid and cathode voltage after the application of an exponentially increasing pulse are shown in Fig. 3.

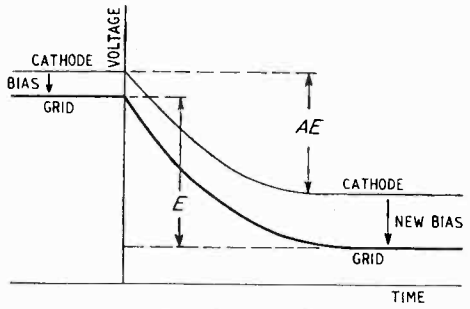

Fig. 3. *Changes in cathode voltage after application of a negative exponential change at the grid.*

If e_{gc} is the initial grid-cathode voltage on the valve just before the application of the pulse then at any time t after the application of a voltage $e = -E(1 - e^{-t/T})$ to the input, the grid-cathode voltage is given by :

$$E_{gc} = e_{gc} + E(1 - A) - \frac{Ee^{-t/T}(1 - T_0/T - A) + AT_0/Te^{-t/T_0}}{1 - T_0/T} \quad (6)$$

where the symbols have the same definitions as in equations (2) and (3).

For the particular case where $T = 0$ (i.e., for a negative step function) we have the conditions indicated in Fig. 4.

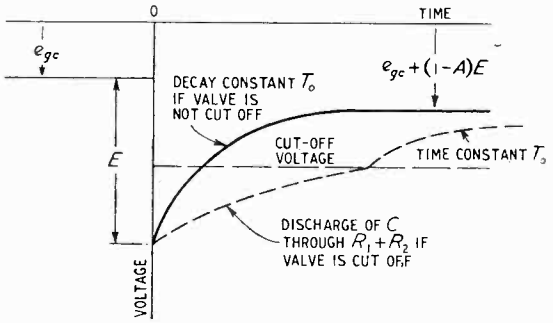

Fig. 4. *Changes in grid-cathode voltage after application of a negative step change of amplitude E.*

If at any time this voltage exceeds the cut-off voltage of the valve, the valve will become an open circuit and the capacitance C will discharge through the resistances R_1 and R_2 until the grid-cathode voltage decreases to the cut-off value, after which decay is at a time constant T_0. This obviously represents considerable distortion of a negative signal.

5. Effect of a Series Grid Resistor

If grid current is limited on positive input pulses by the existence of a series grid resistor, then the cathode-grid voltage is held at a slightly positive value and anode current flow will be limited. Under such conditions it can be shown that (Appendix 2) :—

$$e_{out} = \frac{\mu e_{gc} R}{R + r_a}\left\{1 - \exp\left(-t\frac{R + r_a}{CRr_a}\right)\right\} \qquad (7)$$

for a step function applied at the input.

This rise, which has a time constant much lower than T_0, will continue until the grid-cathode voltage becomes negative, after which the time constant T_0 is applicable.

Fig. 5 shows these changes in cathode and grid voltages. When the step voltage is applied to the input, the grid voltage rises immediately to the cathode voltage, after which the grid and cathode voltages both rise exponentially, the grid being slightly positive with respect to cathode. The difference between the input

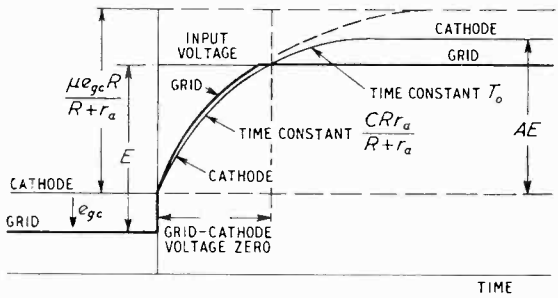

Fig. 5. *Response of cathode voltage with a step function at the input, with high grid circuit impedance.*

and grid voltage appears across the series grid resistor. If the input voltage is E volts, the time at which the input and grid voltages are equal is readily determined, after which the conditions given by equation (7) cease to apply, the grid remaining at the input voltage and the cathode voltage rising with a time constant T_0 until the new operating bias on the valve is developed. The final cathode voltage rise will, of course, be AE, A being the gain of the cathode-follower as defined in equation (2) and E is the applied input voltage.

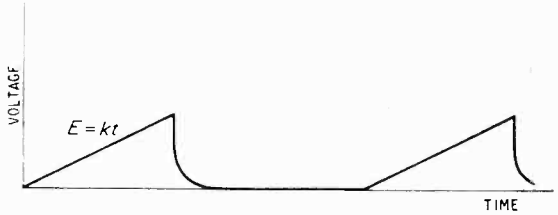

Fig. 6. *A constant change function.*

6. Response to Constant Change Function

We will now consider the response of a cathode-follower to a constant-change function as shown in Fig. 6. This is a common time-base waveform.

If a voltage $E = kt$ is applied to the input, it can be shown that the output voltage is given by :—(Appendix 3.)

$$e_{out} = Ak\{t - T_0\,(1 - e^{-t/T_0})\} \qquad (8)$$

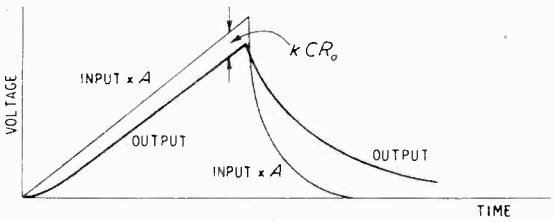

Fig. 7. *Output voltage for input shown in Fig. 6.*

A graph of this function and the input function is given in Fig. 7. It can be seen that after a short time the output voltage is a linear function of time but lags behind the input voltage by an amount which depends on the rate of change of the input voltage and the time constant of the cathode load.

At any time t we have :—

Proportion lag in output voltage =

$$\frac{AE - e_{out}}{AE} = \frac{CR_0}{t}\,(1 - e^{-t/R_0C}) \qquad (9)$$

The exponential term decays rapidly, and AE the output voltage then lags kCR_0 volts behind Akt, the ideal output voltage. The behaviour on the trailing edge is treated in Section 4 above.

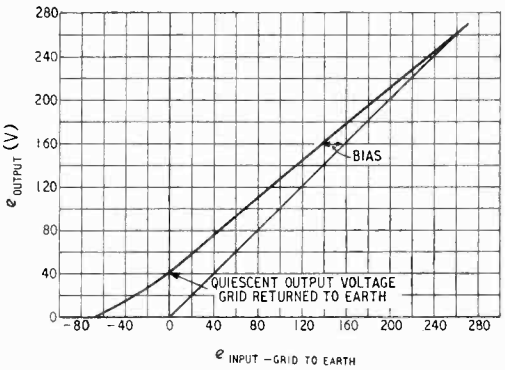

Fig. 8. *Output-input voltages for 6L6 valve with 400-V supply and 4,000 ohms load.*

7. A Typical Example

Consider as an example a cathode-follower consisting of a 6L6 valve with a 400-volt d.c. supply and a cathode load of 4,000 ohms.

The published constants of this valve are :

$g_m = 4.7$ mA/volt

$r_a = 1{,}700$ ohms

$\mu = 8$

$R_m = 1/g_m = 213$ ohms.

From the anode characteristics of the valve, with a loadline of 4,000 ohms, Table I can be prepared.

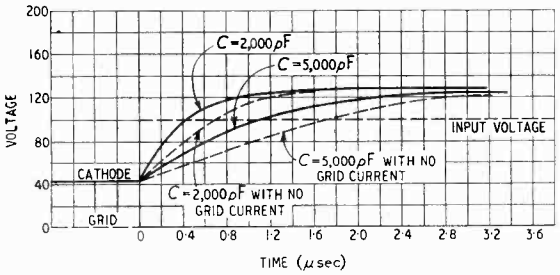

Fig. 9. *Rise of cathode voltage for a step function on the grid.*

TABLE I

Grid Voltage	Anode Current (mA)	Voltage across Valve	Voltage across Load
0	68	130	270
7·5	58	170	230
15	46	216	184
22·5	35	260	140
30	28	288	112
37·5	19	324	76
45	12	352	48
52·5	6	376	24
60	3	382	18
65	0	400	0

The calculated gain is 0.85 and the output impedance is 180 ohms. Fig. 8 is a graph of output voltage against input voltage. For a step function of 100 volts applied to the grid, the cathode voltage for loads of 5,000 and 2,000 pF are given in Fig. 9, the time constant of the output voltages for the two cases are 0.9 μsec and 0.36 μsec respectively, and grid current flows for 1.08 μsec and 0.40 μsec for the two cases. If grid current is limited by the addition of a resistor of, say, 100 kΩ in the grid circuit the output voltages are given by the dotted curves in Fig. 9. The rates of rise are 236 volts per microsecond when grid current flows and 98 volts per microsecond when grid current is limited (2,000 pF load) and 94 V/μsec and 39 V/μsec for the corresponding conditions with a load of 5,000 pF. The response is about 2.4 times as fast when grid current flows.

8. Conclusion

The equations developed and given above enable the performance of cathode-followers under pulse conditions to be calculated. The effect of grid-cathode capacitance has not been considered, but it is hoped to consider this in another article. In general, this capacitance is small compared with the load capacitance and has no effect on the above results.

APPENDIX 1

Change of output voltage for a given input voltage.

Consider the circuits of Fig. 10 :—

Let i be the instantaneous anode current, which has a component i_R in the cathode resistor and i_c in the capacitance

$$i = i_R + i_c$$

we have :—

$$\mu e_g = i_R R + i r_a = i_R R + (i_R + i_c) r_a$$

and

$$\begin{cases} i_c = c \dfrac{de_{out}}{dt} = C \dfrac{d(i_R R)}{dt} = CR \dfrac{di_R}{dt} \\ e_g = e_{in} - i_R R \end{cases}$$

therefore :—

$$\mu(e_{in} - i_R R) = i_R (R + r_a) + CR\, r_a \frac{di_R}{dt}$$

$$CR r_a \frac{di_R}{dt} + i_R\{(\mu + 1) R + r_a\} = \mu e_{in}$$

Assume that the input voltage is an exponential rise function given by $e = E(1 - e^{-t/T})$
This includes as a particular case (when $T = 0$) the step function.

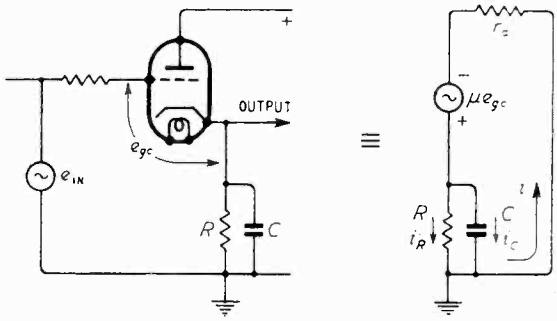

Fig. 10. *Actual and equivalent circuits showing division of anode current between cathode resistor and load capacitance.*

Taking Laplace transforms[1] of both sides we have :—

$$CR r_a\, pI_R + I_R\{(\mu + 1)R + r_a\} = \mu E \left(1 - \frac{p}{p + 1/T}\right)$$

or $I_R = \dfrac{\mu E \left(1 - \dfrac{p}{p + 1/T}\right)}{CR r_a\, p + (\mu + 1) R + r_a}$, where I_R is the transform of current i_R.

$$I_R = \frac{\mu E}{CR r_a\, p + (\mu + 1) R + r_a} - \frac{\mu E p}{(p + 1/T)\{CR r_a p + (\mu + 1) R + r_a\}}$$

[1] The Laplace transforms used here are given in "Applied Mathematics for Engineers and Physicists," L. A. Pipe, McGraw-Hill Book Company. Tables page 130.

Taking inverse transforms :—

$$i_R = \frac{\mu E}{R(\mu + 1) + r_a}\left[1 - \exp\left(-\frac{R(\mu+1)+r_a}{CR\,r_a}t\right)\right] - \mu E \frac{\exp\left(-\frac{R(\mu+1)+r_a}{CRr_a}t\right) - \exp(-t/T)}{\frac{CRr_a}{T} - R(\mu+1) - r_a}$$

If we introduce the well-known formulae for gain and output impedance :—

$$A = \frac{\mu R}{(\mu + 1)R + r_a}$$

$$R_o = \frac{r_a R}{(\mu + 1)R + r_a}$$

and putting $T_0 = CR_0$ we have :—

$$e_{out} = i_R R = AE(1 - e^{-t/T_0}) - AE\frac{(e^{-t/T_0} - e^{-t/T})}{T_0/T - 1}$$

$$= AE\left\{1 - \frac{T_0 e^{-t/T_0} - Te^{-t/T}}{T_0 - T}\right\}$$

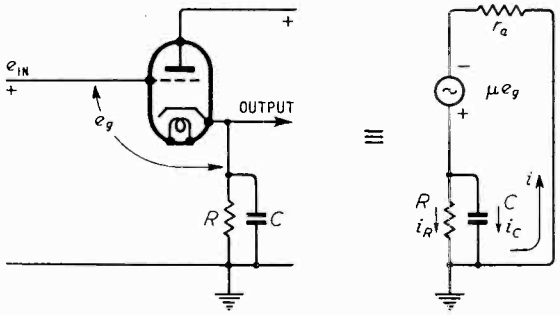

Fig. 11. *Actual and equivalent circuits with series grid resistor.*

APPENDIX 2

Conditions existing when grid is prevented from drawing current.

We have the equivalent circuit of Fig. 11.

If there is a large series grid resistor, then if e_{gc} is the bias on the valve before the application of the input pulse, we have:—

$$\mu e_{gc} = i_R R + (i_R + i_c) r_a$$

$$i_c = CR\frac{di_R}{dt}$$

$$\therefore CRr_a\frac{di_R}{dt} + i_R(r_a - R) = \mu e_{gc}$$

Taking Laplace Transforms :—

$$I_R = \frac{\mu e_{gc}}{CRr_a p + r_a + R}$$

which yields a solution

$$i_R = \frac{\mu e_{gc}}{r_a + R}\left[1 - \exp\left(-\frac{R + r_a}{CRr_a}t\right)\right]$$

or $e_{out} = \frac{\mu e_{gc} R}{R + r_a}\left[1 - \exp\left(-\frac{R + r_a}{CRr_a}t\right)\right]$

This will hold until the grid becomes negative, after which the time constant T_0 is applicable, as shown in Fig. 5.

APPENDIX 3

Response of cathode-follower to a constant change function.

Here equation (1) in the text is applicable and e_{in} is equal to kt.

Thus we have :—

$$r_a CR\frac{di_R}{dt} + i_R\{(\mu + 1)R + r_a\} = \mu kt$$

Taking Laplace transforms of both sides we have :—

$$r_a CR\,pI_R + I_R\{(\mu + 1)R + r_a\} = \frac{\mu k}{p}$$

$$\text{or } I_R = \frac{\frac{\mu k}{r_a CR}}{p\left(p + \frac{(\mu + 1)R + r_a}{r_a CR}\right)}$$

where I_R is the Laplace transform of the current i_R Taking inverse transforms we have :—

$$i_R = \frac{\mu k}{r_a CR}\left[\frac{tr_a CR}{(\mu + 1)R + r_a} - \frac{(r_a CR)^2}{\{(\mu + 1)R + r_a\}^2}\left\{1 - \exp\left(-\frac{(\mu + 1)R + r_a}{r_a CR}t\right)\right\}\right]$$

gives the output voltage as a function of time.

If we again introduce the formulae for gain A and output impedance R_0, as given in Appendix 1, we have :—

$$e_{out} = Ak[t - R_0 C(1 - e^{-t/R_0 C})]$$

$$e_{out} = Ak[t - T_0(1 - e^{-t/T_0})]$$

which gives the output voltage as a function of time, the ideal output voltage (when $C = 0$) being Akt or A times the input voltage.

INTERFERENCE IN MULTI-CHANNEL CIRCUITS

Dependence on Harmonic Generation

By L. Lewin

(*Standard Telecommunication Laboratories*)

SUMMARY. On the assumption that the relation between output and input for any unit of the link can be represented as a power series of the input signal, suitably delayed, the harmonic content of the output for a pure tone input signal is found. When a multi-channel signal is injected it is found that the inter-channel interference falling in any particular channel consists of a number of separate terms, each bearing a functional relation to a corresponding harmonic component of the output when a pure tone test signal is used as input. This relation is found in the form of an integral in which the r.m.s. amplitude of the pure tone input occurs as a variable of integration. Hence, to find the interference level, the harmonics have to be measured over a range of values of input amplitude, and the interference components deduced by a somewhat involved analysis. Only in the case in which the second and third harmonics predominate is this procedure unnecessary, and there is then a direct and simple relation between interference and harmonics. This latter construction confirms the standard procedure for finding the interference level in this region. Otherwise, the paper is at variance with other published work, in that the latter neglects the effects of coherence, which are here considered in detail.

A particular case—distortion due to mis-matches on a long feeder line—is investigated in detail, and it is shown that, for increasing feeder length, the interference and second harmonic at first increase together, but that, for long feeder lengths, the former decreases slowly while the latter passes through a maximum and then oscillates, its place as the dominant harmonic being taken first by the third, and then successively by higher harmonics. It is shown that, in this example, both the second and third harmonics could vanish for certain feeder lengths, although the interference could remain at an appreciable level, so that caution is necessary before accepting small absolute values of harmonics at their face value. In this connection, the importance of small variations of feeder length or of carrier frequency in determinations of interference levels, is stressed.

It is shown that the beat-frequency method of harmonic measurement, at present in use, although convenient from several points of view, is not exactly equivalent to a determination of the harmonic levels and cannot be used for the analysis of this paper. The two methods are equivalent, however, when the second and third harmonics can be shown to be the only significant ones, in which case, as already stated, the relationship with the interference level is straightforward.

1. Introduction

ONE of the most important characteristics of the performance of a multi-channel link is the inter-channel interference level. It is not normally possible to measure this directly in test, as a suitable multi-channel source is not likely to be available. Instead, a pure tone signal can be injected, and the harmonic margin measured. This harmonic level is then usually taken as an indication of the interference level to be expected from the working link. The purpose of this paper is to examine in detail the connection between the harmonic level on the one hand, and the performance of the link on the other, and to suggest a precise test procedure for relating the two.

2. Harmonic Production

We shall confine ourselves, for the most part, to the multi-channel signal, which will be at 'video' frequency. In this band it will be assumed that the relation between output and input signals for any unit of the link can be represented by a power series

$$V = a_1 s + a_2 s^2 + \ldots \qquad (1)$$

MS accepted by the Editor, January 1950

where $s = s(t)$ is the input signal, either multi-channel, or test. There will in general, be a time delay τ, so that s in Equ. (1) is really $s(t - \tau)$. This delay can be ignored provided, of course, it is the same delay which occurs in each power of s. An exception can be made, however, for the term $a_1 s$, which represents the recovered signal, and which will normally be much larger than the other (distortion) terms. Since we are concerned with the distortion level relative to the recovered signal level, it is only the amplitude of the latter which is of interest so that its phase can be ignored. But all of the distortion terms combine together to give the various harmonics, and hence their relative phase is important.

In what follows, it will be understood, to save repetition, that all harmonic and interference levels are referred to their respective signal levels.

If we put $s = x\sqrt{2}\cos qt$, to represent a pure tone test signal, into Equ. (1), x being the r.m.s. level, we get

$$V = a_1 x\sqrt{2}\,[\cos(qt) + \sum_{2}^{\infty} f_n(x)\cos(nqt)] \qquad (2)$$

The amplitude $f_n(x)$, which is a function both of the coefficients of Equ. (1) and the r.m.s. value

of the signal, x, is obtained in Appendix 1. It represents the harmonic margin of the n^{th} harmonic of frequency nq, and is the quantity which can be measured in a straightforward way in test. For example, if with a certain input signal level, $f_2(x)$ is measured as 10^{-3}, then the second harmonic is $20 \log_{10}(10^{-3}) = 60$-db down on the recovered signal (which appears, of course, in a different part of the band).

The harmonic amplitudes $f_n(x)$ vary with the r.m.s. input signal amplitude, x, and all obviously vanish at $x = 0$. Their actual behaviour as x varies turns out to be important in relating them to the inter-channel-interference level.

3. Multi-Channel Signal

Let there be N channels (N large) equispaced in frequency by an amount p c/s, so that the 'video' frequency of the n^{th} channel is np. Then a multi-channel signal can be represented by

$$S = x\sqrt{2/\alpha N} \sum_{1}^{N} \epsilon_n \cos(npt + \theta_n) \quad \ldots \quad (3)$$

It is here assumed, for simplicity, that the channels start at $n = 1$, but the ensuing analysis may be used if a small number at the bottom are missing, provided N is increased by a corresponding amount.

θ_n is a random phase angle, which ensures incoherence between different channels. ϵ_n is a quantity which is 1 or 0 according to whether the n^{th} channel is working or not.

We assume $\sum_{1}^{N} \epsilon_n = \alpha N$, so that α is the fraction of channels actually transmitting at any given moment. (Approximately, half the channels will not be in use, owing to waiting, dialling, etc., while of those in use, roughly a half will be listening, and therefore not transmitting. α may therefore be taken to be about a quarter.)
Since $\epsilon_n^2 = \epsilon_n$ (both being either 0 or 1), the r.m.s. of the signal of Equ. (3) is

$$\sqrt{(2x^2/\alpha N) \sum_{1}^{N} \tfrac{1}{2}\epsilon_n^2} = \sqrt{(2x^2/\alpha N)\tfrac{1}{2}\alpha N} = x.$$

However, the signal level of a working channel is $x\sqrt{2/\alpha N}$, and it is to this level that the interference will be referred.

4. Generation of Inter-channel Interference

Let us confine our interest to the r^{th} channel, and define a quantity $y = r/N$; y defines the position of the r^{th} channel, is zero at the bottom, and 1 at the top of the band of channels.

Let us substitute in Equ. (1) the multi-channel signal of Equ. (3), multiply out, and convert products of cosine terms to sum and difference terms. All those whose resultant frequency falls in the r^{th} channel can be picked out, and constitute the interference in that channel.

At first sight it would appear that all such terms would be incoherent, thus adding up 'power-wise' to give the total interference, but this is not the case. A detailed analysis reveals that they fall into groups with a certain amount of coherence within a group, and with no term in any one group coherent with any term in any other group. The amplitude of the n^{th} group is denoted by $g_n(x)$ and is a function of the r.m.s. amplitude x, of the multi-channel signal of Equ. (3). $g_n(x)$ is related, though not in a very simple way, to the function $f_n(x)$ discussed in Section 2. For this reason $g_n(x)$ can conveniently be referred to as the n^{th} harmonic component of the interference. It should be understood, however, that this nomenclature is only by analogy with $f_n(x)$, and is not intended in any way to describe the method of formation of the group. As described above, each group is generated by beat frequencies of all orders and from all channels, and it is, perhaps, a matter of surprise that there is such a definite segregation of terms into groups.

5. Relation Between $g_n(x)$ and $f_n(x)$

We are interested in the r^{th} channel, and in order to find the harmonics produced in this channel by a pure tone input of frequency q, we take $q = \frac{1}{2}rp$ for the second harmonic, $q = \frac{1}{3}rp$ for the third, and so on. Then an input of $x\sqrt{2}\cos(rpt/n)$ will produce in the r^{th} channel its n^{th} harmonic of amplitude $f_n(x)$ (relative to the fundamental which appears, of course, in the channel r/n). It is this quantity $f_n(x)$ which will be related to that part of the component of interference $g_n(x)$, which falls in the r^{th} channel. $g_n(x)$, as already stated, is referred to the level of the channel signal, so that, when it is found, the total interference margin $G(x)$ in the r^{th} channel, can be found from $G^2(x) = \sum_{2}^{\infty} g_n^2(x)$.

The power-wise addition follows from the mutual incoherence between the groups. $G(x)$ will, of course, also be a function of $y = r/N$ which gives the channel position, so that the interference will, in general, vary (smoothly) from channel to channel. Normally, only the first few harmonics $f_n(x)$ will be significant, so that the number of $g_n(x)$ to be summed is correspondingly few.

In Appendix 2 it is shown that

$$g_2(x) = \sqrt{4\alpha(1 - y/2)}\cdot\frac{1}{x^5}\int_0^\infty f_2(z)e^{-z^2/x^2}z^4dz \qquad (4)$$

4α can usually be replaced by unity, while the factor $\sqrt{1 - y/2}$ shows a variation of 0.7 : 1 ≡ 3 db from the top to the bottom of the band of channels. For the r^{th} channel we simple insert the value of $y = r/N$. To calculate $g_2(x)$, which is the amplitude of the second-harmonic component of interference for the r^{th} channel, it is first necessary to measure $f_2(z)$ over as wide a range of r.m.s. amplitude, z, as the experimental procedure may permit. A single tone of frequency $\frac{1}{2}rp$ is injected, and its r.m.s. varied as just described. The value of harmonic appearing in the channel r referred to the fundamental appearing in the channel $r/2$ is the function $f_2(z)$ required. This value must be inserted into Equ. (4), into which has also been put the correct value of x, the r.m.s. value at which the total muli-channel signal is intended to operate.

The integration may be performed graphically; or by fitting the measured $f_2(z)$ with a polynomical of the form $b_1z + b_3z^3 + b_5z^5 + \ldots$ only odd powers appearing. In either case, it is necessary to check that the largest value of z which has been reached is sufficient for the factor e^{-z^2/x^2} to have reduced the integrand to a small enough value to justify neglecting the contribution from the rest of the range. It is easily shown that

$$\int_0^\infty z^{2n+1}e^{-z^2/x^2}dz = n!\,x^{2n+2}/2, \quad \text{whence we}$$

have the following particular values.

$$\int_0^\infty z^5e^{-z^2/x^2}dz = x^6; \quad \int_0^\infty z^7e^{-z^2/x^2}dz = 3x^8;$$

$$\int_0^\infty z^9e^{-z^2/x^2} = 12x^{10}; \quad \int_0^\infty z^{11}e^{-z^2/x^2}dz = 60x^{12};$$

$$\int_0^\infty z^{13}e^{-z^2/x^2}dz = 360x^{14}; \text{ etc.}$$

Hence, when $f_2(z) = b_1z + b_3z^3 + b_5z^5 + \ldots$ we get

$$g_2(x) = \sqrt{4\alpha(1 - y/2)}[b_1x + 3b_3x^3 + 12b_5x^5 + \ldots] \qquad (5)$$

In particular, when x is small enough, it is seen that, apart from the factor $\sqrt{4\alpha(1 - y/2)}$, the first terms of g_2 and f_2 are the same. Hence, for sufficiently small values of x we have

$$g_2(x) \approx \sqrt{4\alpha(1 - y/2)}f_2(x), \; x \text{ small} \qquad (6)$$

The order of approximation is that the fourth and higher harmonics be negligible compared to the second. Unless this is so, the full Equs. (4) or (5) must be used. When Equ. (6) can be used it is not necessary, of course, to measure $f_2(x)$ over a range of values since the integration of Equ. (4) is no longer called for.

The function $g_3(x)$ is similarly found to be given by

$$g_3(x) = \sqrt{4\alpha(1 - y^2/3)/2}\,\frac{1}{x^6}\int_0^\infty f_3(z)e^{-z^2/x^2}z^5dz \qquad (7)$$

As before, $f_3(z)$ must be measured over a range of values of z, a fundamental of frequency $rp/3$ being used. $f_3(z)$ is obtained by referring the amplitude of the 3rd harmonic appearing in the r^{th} channel to the fundamental which now appears in the channel $r/3$. $f_3(z)$ can be fitted by the expansion $b_2z^2 + b_4z^4 + b_6z^6 + \ldots$, giving

$$g_3(x) = \sqrt{4\alpha(1 - y^2/3)/2}\,[3b_2x^2 + 12b_4x^4 + 60b_6x^6 + \ldots] \qquad (8)$$

When x is small enough we get the approximation, from the first term only,

$$g_3(x) \approx (3/\sqrt{2})\sqrt{4\alpha(1 - y^2/3)}f_3(x), \; x \text{ small} \qquad (9)$$

The order of the approximation is the same as for Equ. (7). When this is satisfied, the higher g_n are then negligible, so that we have the approximation

$$G(x) \approx \sqrt{4\alpha[(1 - y/2)f_2^2(x) + (9/2)(1 - y^2/3)f_3^2(x)]}, \; x \text{ small} \qquad (10)$$

In general,

$$g_n(x) = [\sqrt{4\alpha h_n(y)}/x^{n-3}]\int_0^\infty f_n(z)e^{-z^2/x^2}z^{n-2}dz$$

$$\text{with } h_n(y) = \frac{2^n}{\pi\, n!}\int_0^\infty \cos y\theta\left(\frac{\sin\theta}{\theta}\right)^n d\theta \qquad (11)$$

Particular values are

$h_2(y) = 1 - y/2$; $h_3(y) = (1 - y^2/3)/2$;
$h_4(y) = (8/9 - y^2/3 + y^3/12)/4$;
$h_5(y) = (46 - 12y^2 + 6/5y^4)/(24)^2$

$f_n(z)$ may be approximated by a polynomial commencing with the term $b_{n-1}z^{n-1}$, successive terms having exponents of z increasing by 2. The integrations can, of course, be done graphically.

6. Comparison with Published Results

Comparison will here be made with the paper by Brockbank and Wass[1], which treats all orders of distortion in some detail. Although the approximate formula (10) above is in general agreement with the results of the same order in the above paper, there is no reference there to the semi-coherent groups, $g_n(x)$, and their relation to $f_n(x)$. The reason can be found in the paragraph (9.3) " Low-Order Products from High-Order terms " in which it is stated " It can be shown that, although the power in each such low-order product may exceed the power in each higher order product, the number of products is

so much lower when N is not small that the total distortion power in the higher order products is considerably greater than the power in the lower-order products." They have, therefore, neglected these low-order products. What has not been realized is that these low-order products are *coherent* with other terms that are not negligible, and that these terms and the low-order products will therefore add up voltage-wise and not power-wise. The effect, as found here, is to make the effects of the low-order and high-order products of the same order of magnitude, so that agreement is limited to the region in which all such products can be neglected. This leads to Equ. (10).

As stated above, the occurrence of coherent groups is quite unexpected, and they can only be determined by a very detailed analysis. That they must occur is apparent when it is realized that such a term as, for example $(A + B - C)$ in a third-order product, is repeated identically in frequency *and phase* in a fifth-order product which gives such a term as $(A + B - C + D - D) = (A + B - C)$. The writer is not aware if such an effect has already been treated in the literature, but it seems necessary that when higher-order harmonics have to be treated, that the analysis follow closely that outlined here.

7. Coherence with the Main Signal

The odd-harmonic interference components are peculiar in that part of each of them undergoes a phase change of exactly ϕ when each individual term undergoes this same change. Thus if we consider the expanded form of the product $\cos(lpt + \phi) \cos(mpt + \phi) \cos(npt + \phi)$ one of the terms will be of the form $\cos\{(lpt + \phi) + (mpt + \phi) - (npt + \phi)\} = \cos\{(l + m - n)pt + \phi\}$ which is seen to have changed by the same amount ϕ. If the main signal also undergoes this same change ϕ, it follows that part of the interference terms remain in phase with the main signal, and hence will add up voltage-wise rather than power-wise as the signals are transmitted from repeater to repeater. *In any particular case, however, it must be checked whether the main signal really does alter by the same phase angle, as even a small variation will destroy the coherence effect.* In the next section an example is treated in which a phase difference actually is introduced between the main signal and the interference components, such that the odd-harmonic components no longer give coherence with the main signal.

As an example of the separation of cross-talk components let us investigate the third-harmonic component of interference $\bar{g}_3(x)$. Then it is shown in the Appendix

$$\bar{g}_3(x) = \sqrt{\alpha(1 + 2y - 2y^2)}\,\frac{1}{x^6}\int_0^\infty f_3(z)e^{-z-\alpha z^2}z^5 dz$$

Hence

$$\bar{g}_3(x)/g_3(x) = \sqrt{(1 + 2\nu - 2\nu^2)/2(1 - y^2/3)} \qquad (11)$$

a result that depends only on the position, y, of the channel. The right-hand side of Equ. (11) varies from 0.71 at $y = 0$ to a maximum of 0.92 at $y = 0.7$ and down to 0.87 at $y = 1$. Thus nearly the whole of $g_3(x)$ is of this 'in phase' type, and may add up voltage-wise from repeater to repeater.

8. Distortion from a Mis-matched Feeder

Unless the analytic form of the output of Equ. (1) is known, the general analysis cannot be taken any further, and the results so far presented are intended for application when the various functions $f_n(x)$ have been determined experimentally.

However, a particular case which is capable of complete treatment is that caused by phase distortion due to a mis-matching at the end of a long feeder line. In a previous paper[2] on this subject the function $f_n(x)$ for this case was determined.

A frequency-modulated signal is transmitted from a long feeder, but owing to mis-matches at its ends, multiple reflections are set up within the feeder. These cause a phase distortion of the transmitted wave, and in Equ. (3) the expected output is shown to be given by

$$V = \Delta\omega \sin(\omega_a t) - \delta$$

$$\delta = \frac{d}{dt}[kr_1r_2 \sin(2\omega_c\tau - \theta_1 - \theta_2 + 2\tau\Delta\omega \cdot \sin(\omega_a t - \tau) \sin(\omega_a\tau)/\omega_a\tau)] \qquad (13)$$

Here, ω_c is the r.f. carrier and $\Delta\omega \sin \omega_a t$ is the pure tone input signal, which is recovered together with distortion terms; the latter are represented by the second term in Equ. (13). r_1 and r_2, and θ_1 and θ_2 are respectively the amplitudes and phase angles of the reflection coefficients at each end of the feeder. τ is the time delay along the feeder, and equals l/v where l is the feeder length and v the group velocity of the waves. k is the attenuation along the double length of feeder and equals $e^{-2\alpha l}$ where α is the attenuation coefficient.

Equ. (13) has to be compared with Equ. (1) with $s = \Delta\omega \sin \omega_a t$—the r.m.s. amplitude x being given by $\Delta\omega = x\sqrt{2}$. It is seen that Equ. (13) as it stands is not capable of expansion in powers of s, owing to (1) the presence of $\sin(\omega_a\tau)/\omega_a\tau$, which contains ω_a, a characteristic of the signal: (2) the occurrence of $t - \tau$ instead of t in the

distortion terms, and (3) the operator d/dt. ω_a is the video frequency and is usually not very high so that unless the feeder run is so large that it becomes comparable with the wavelength of the video-frequency, $\omega_a\tau$ will be small. Hence $\sin(\omega_a\tau)/\omega_a\tau$ can be replaced by unity without serious effect, and point (1) above is no longer a limitation.

Point (2) is covered by Section (2), which permits all powers of s above the first to contain a constant delay. However, since the recovered signal in Equ. (13) contains no delay, the distortion terms, although coherent with the main signal, will differ in phase from it by an angle $\omega_a\tau$. (That such a delay must occur is apparent when it is realized that the distortion terms arise from waves that have been reflected down the feeder and back again before transmission). Hence the 'in-phase' components of odd-order interference harmonics, although coherent with the main signal, are not actually in phase with it, and the phase difference changes from repeater to repeater, giving the appearance of a random phase change. Thus for all practical purposes, this component behaves as if it were incoherent, and there is no call to extract it from the rest of the interference terms for special treatment. It will not add up voltage-wise from repeater to repeater.

So far as the operator d/dt is concerned, if it were applied at the end of the analysis, no alteration would be called for. It would produce merely a factor, which for Equ. (13), would be $n\omega_a$ for the n^{th} harmonic; and which, in the multi-channel case, would be rp for the r^{th} channel. Hence, if we quote results in which d/dt has been applied at an earlier stage, the only change necessary is the replacement of $n\omega_a$ by rp.

The functions $f_n(x)$ for this problem are easily obtained from Equ. (13) by the Fourier-Bessel expansion, and are given in Equ. (5) of the paper referred to. Replacing $n\omega_a$ by rp as discussed above we get

$$f_n(x) = kr_1r_2(rp)\frac{J_n(x2\sqrt{2\tau})}{x}\left[\sqrt{2}\begin{matrix}\sin\\ \cos\end{matrix}(2\omega_c\tau - \theta_1 - \theta_2)\right] \quad .. \quad (14)$$

The sin or cos occurs according to whether n is even or odd. Since the phase angle $2\omega_c\tau - \theta_1 - \theta_2$ is indeterminate without a precise knowledge of the particular arrangement in use, we can, in considering over-all behaviour of many units, replace the terms in square brackets by their r.m.s., in this case unity. However, this is only an average effect, and for any particular feeder at any one repeater this term will be quite definite, and only if $2\omega_c\tau - \theta_1 - \theta_2$ reduces to 45° will the results be the same. But the effects of different repeaters, or of the same repeater under slightly different conditions of temperature, etc., can be simulated by a variation of $\omega_c\tau$. This can be conveniently done either by small changes of ω_c or by varying τ, by means of a line lengthener. In the ensuing analysis the results will be averaged out by taking the r.m.s. for the indeterminate phase term, but the above statement must be borne in mind in the interpretation of any single result.

Accordingly, we take for $f_n(x)$

$$f_n(x) = kr_1r_2(rp)J_n(x2\sqrt{2\tau})/x \quad .. \quad (15)$$

The integrations required by Equ. (11) can be performed by means of the following integral[3]

$$\int_0^\infty J_n(at)e^{-b^2/x^2}t^{n+1}dt = a^n\left(\frac{x^2}{2}\right)^{n-1}e^{-a^2x^2/4}$$

Hence, using Equs. (11) and (15), we get

$$g_n(x) = \frac{kr_1r_2(rp)}{x^{n+3}}\sqrt{4\alpha h_n(y)}\int_0^\infty J_n(z2\sqrt{2\tau})z^{n+1}e^{-z^2/x^2}dz = k\sqrt{4\alpha h_n(y)}r_1r_2(rp)x^{n-1}\tau^n 2^{(n/2-1)}e^{-2\tau^2x^2} \quad .. \quad .. \quad (16)$$

The total cross-talk power in the r^{th} channel is

$$G^2(x) = \sum_2^\infty g_n^2(x) = \frac{4\alpha}{\pi}(kr_1r_2rp\tau)^2e^{-4\tau^2x^2}\int_0^\infty \cos y\theta \sum_2^\infty\left(\frac{\sin\theta}{\theta}\right)^n\frac{(2\tau x)^{2n-2}}{n!}d\theta \quad (17)$$

on replacing $h_n(y)$ by its value as given by Equ. (11).

Summing, and taking the square root, we get for the total interference amplitude

$$G(x) = \sqrt{\alpha}kr_1r_2(y\omega_N)e^{-2\tau^2x^2}\phi(\tau x)/2x$$

where

$$\phi(\tau x) = \left[\frac{4}{\pi}\int_0^\infty \cos y\theta\left\{\exp(4\tau^2x^2\sin\theta/\theta) - 1 - 4\tau^2x^2\sin\theta/\theta\right\}d\theta\right]^{\frac{1}{2}} \quad .. \quad (18)$$

Here, we have put $rp = \frac{r}{N}\cdot Np = y\omega_N$ where $\omega_N = Np$ is the angular frequency (video) corresponding to the top of the multi-channel band.

The integral in (18) cannot be evalulated in closed form, but very good approximations for the top and bottom of the band ($y = 1$ and 0) are found in Appendix 3. The variation (for the integral) is always less than $1:\sqrt{2}$ over the video band, and since the form is much simpler at the top, we will confine our attention there. However, it is seen from Equ. (18) that apart from this slow variation, $G(x)$ is also proportional to y, so that the interference *from the causes investigated*

in this example vanish at the bottom channels of the band.

Using the approximations of Appendix 3 for the top of the video band, we find the interference level in the top channel:

$$G(x)_{y=1} = G_1 \text{ (say)} \approx \sqrt{\alpha} r_1 r_2 \omega_N \sqrt{1 - (1 + 4\tau^2 x^2) \exp(-4\tau^2 x^2)}/2x, \quad (\tau x < 1) \quad \ldots \quad (19)$$

For larger feeder lengths

$$G_1 \approx \sqrt{\alpha} r_1 r_2 \omega_N \frac{1.175}{2x} \sqrt{\frac{1 - 0.32/(\tau x)^2}{\tau x}}, \quad \tau x > 1 \quad \ldots \quad (20)$$

For very short feeders, Equ. (19) gives

$$G_1 \approx \sqrt{2\alpha} r_1 r_2 \omega_N \tau^2 x, \quad \tau x < 0.3 \quad \ldots \quad (21)$$

The actual curve as a function of τx is shown in Fig. 1.

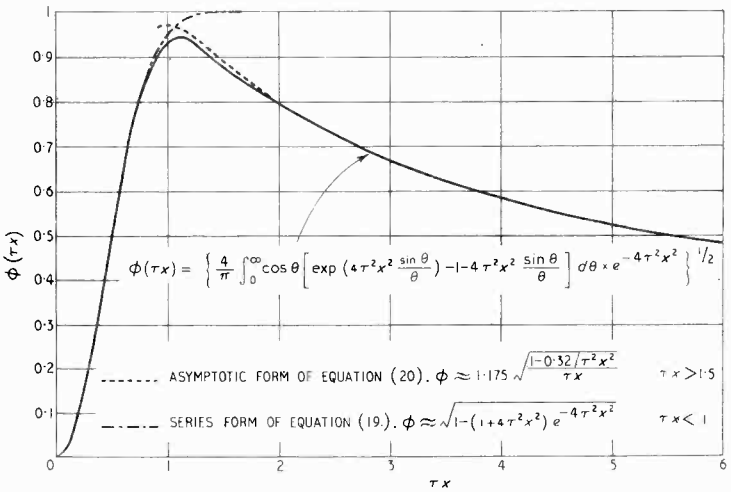

Fig. 1. *Interchannel interference produced in a mis-matched feeder.*

As an example, consider a feeder 55ft long, with a system in which the r.m.s. frequency deviation is 2 Mc/s. Assume the r.f. feeder is a waveguide in which the group velocity of the waves is 0.7 light velocity. Then $\tau x = 2\pi \times 55 \times 12 \times 2.54 \times 2 \times 10^6 \times 1/(0.7 \times 3 \times 10^{10}) = 1$. This is at the transition between Equs. (19) and (20) for which the two functions of τx at $\tau x = 1$ are respectively 0.95 and 0.97. The correct value, used in obtaining Fig. 1, is 0.925 from the series expansion. It follows that, for this example, we can use the asymptotic form of Equ. (20) for runs longer than about 60ft, the interference amplitude for such lengths dropping roughly as the inverse square root of the feeder length.

If ω_N is 0.8 Mc/s and r_1 and r_2 correspond to standing-wave ratios of 0.95 and 0.8, we get, neglecting attenuation ($k = 1$).

$$G = \sqrt{\frac{1}{4}} \times \frac{1-0.95}{1+0.95} \times \frac{1-0.8}{1+0.8} \times \frac{0.8}{4} \times 0.925 = 0.263 \times 10^{-3}.$$

Thus the interference is about 72-db down. This is some 7-db better than that obtained from Equ. (3) of Reference 2, from a consideration of the 2nd harmonic only.

For $\tau x = 1$, the ratio of 3rd to 2nd harmonic, when each in turn is arranged to occur at the top of the band, is $J_3(2\sqrt{2})/J_2(2\sqrt{2}) = 0.28/0.48 = 0.56$, so that the second harmonic can no longer be considered dominant. For values of τx greater than 1; $J_2(2\sqrt{2}\tau x)$ decreases, passing through zero when $\tau x = 1.8$, while the third, and subsequently the fourth and higher harmonics 'take over'. The interference decreases monotonically for values of τx greater than 1, and there is no simple direct relation between it and the various harmonics, apart from the already mentioned approximate equality to the second harmonic, when the latter is the dominant one.

It should be emphasized again that the behaviour described above is an *average* one, averaged for different values of the normally indeterminate phase angle $2\omega_c\tau - \theta_1 - \theta_2$. For a particular set-up, this quantity may, for example, be a multiple of π, so that

$$\sin(2\omega_c\tau - \theta_1 - \theta_2) = 0.$$

In this case there would be no second harmonic at all—and the interference would be correspondingly reduced—but such an example would not adequately describe the characteristics of the unit, since the next one might well have a large second harmonic—and interference level—consequent on a different value of the phase. The only way to obtain significant results is, as mentioned previously, to conduct the test over a range of values of phase (by varying ω_c or l) and to take the average of the results. This should then lead to the *average* harmonic levels and interference levels of Equs. (15) and (19) respectively.

9. Recommended Test Procedure

In order to estimate the interference level in the r^{th} channel, of video frequency rp, the following procedure is suggested:

(1) Inject a signal of frequency $rp/2$ and r.m.s. amplitude z, and measure the level of harmonic appearing in the r^{th} channel relative to the signal appearing in channel $(r/2)$. Vary z from zero to as large a value as the experiment may permit. Then the relative harmonic amplitude is $f_2(z)$ as defined in Equ. (2).

(2) Calculate $g_2(x)$ from $f_2(z)$ by means of Equ. (4). In this derivation the r.m.s. level at which it is intended to work the total video signal in the link is presumed known. α may usually be taken as 1/4. The integration may either be performed graphically or by fitting $f_2(z)$ with a polynomial $b_1z + b_3z^3 + b_5z^5 + \ldots$ From Equ. (5) the value of $g_2(x)$ is $\sqrt{4\alpha(1-y^2/2)}$ $[b_1x + 3b_3x^3 + 12b_5x^5 + \ldots]$

(3) Repeat (1) but use a fundamental of frequency $rp/3$. The signal appears in channel $(r/3)$ and its third harmonic in channel r. The ratio of the amplitudes is $f_3(z)$.

(4) Derive $g_3(x)$ from $f_3(z)$ using Equ. (7). If $f_3(z)$ is fitted by $b_2z^2 + b_4z^4 + b_6z^6 + \ldots$ then, from Equ (8)

$$g_3(x) = \sqrt{4\alpha(1 - y^2/3)}\,/2$$
$$[3b_2x^2 + 12b_4x^4 + 60b_6x^6 + \ldots]$$

(5) Repeat the above measurements for the higher harmonics using a fundamental of frequency rp/n and deduce $g_n(x)$ from $f_n(z)$ by Equ. (11).

(6) The total interchannel interference power level G^2 is given by

$$G^2 = g_2^2(x) + g_3^2(x) + g_4^2(x) + \ldots$$

As explained in Section (7) it may be necessary to make a partial separation of the odd harmonics, to allow for the 'in-phase' effect.

(7) Repeat the above steps with slightly different carrier frequencies or feeder lengths, to simulate the effects of repeater variations.

If it can be shown that only the second and third harmonics are significant, then it is permissible to avoid most of the above analysis, and use simply Equs. (6) and (9) which give

$$\left.\begin{aligned} g_2(x) &\approx \sqrt{4\alpha(1-y/2)}\,.\,f_2(x) \quad .. \quad .. \\ g_3(x) &\approx \frac{3}{\sqrt{2}}\sqrt{4\alpha(1-y^2/3)}\,.\,f_3(x) \quad .. \\ G^2 &\approx g_2^2(x) + g_3^2(x) \end{aligned}\right\} \quad (22)$$

The measurement of $f_2(x)$ and $f_3(x)$ over a range of values of r.m.s. amplitude is not necessary here, and only the actual amplitude which it is intended to use in the working link is needed.

In deciding whether or not the second and third harmonics are the only ones of value, absolute smallness of these is not in itself a reliable criterion, although it may often be correct. For example, in the application given in Section 7, the second harmonic could be small either on account of the feeder phase being nearly a multiple of π, or because the length of feeder was actually such as to bring $x\tau$ of Equ. (15) into the region giving low second harmonic, the third or higher harmonics being dominant. In the first case the smallness could be reflected in a low value of interference, albeit this effect would not be repeatable from repeater to repeater on account of the feeder phase angle not being exactly determinate. In the second case the small value of second harmonic could be misleading. If we had $\tau x = 1.8$ and $2\omega_c\tau - \theta_1 - \theta_2 = n\pi + \pi/2$, both second and third harmonic would be zero, although the interference in this case would be near its maximum. On the other hand, if kr_1r_2 were very small (feeder well matched) the second and third harmonics would be small and this would be 'genuine' in that the interference would be correspondingly small. Caution is therefore necessary before accepting low values of second and third harmonics at their face value.

10. Alternative Test Procedure

Since the bottom channel may, in practice, start somewhere around $r = 15$ instead of $r = 0$, it is not possible to carry out the above analysis too far, or over the whole of the band, as either the fundamental or its harmonics may be outside the range of the apparatus at one end of the band or the other. Hence an alternative method is in use in which a double-tone signal is injected and difference frequencies are looked for. This method has the advantage of being usable over the whole band. So long as only the second and third harmonics (of the single-tone test) are significant, the two methods give the same results, and the order of approximation is the same as that which leads to Equ. (22) above.

However, if higher-order harmonics than the third cannot be neglected, it is easy to see that the beat-frequency method no longer gives the various harmonics accurately, any more than $f_2(x)$ can give $g_2(x)$ directly, as in the approximations of Equ. (22). The order of errors is probably the same in both cases, so that it is pointless to try to use the preceding analysis without the use of the correct functions $f_n(x)$ [except, as already stated, to the approximation of Equ. (22)]. There is, of course, a relation between the harmonic amplitudes $f_n(x)$ on the one hand, and the beat-frequency measurements on the other, but they certainly are not of any simple form. It is hoped to investigate this at a later date. Meanwhile, if the full analysis of this paper is

called for in any particular arrangement, there seems to be no alternative to the full procedure of Section (9) with its necessary limitations.

11. Conclusions

Although the general validity of existing test practice is confirmed in the case in which the second and third harmonics can be shown to be the only significant ones, caution is necessary in accepting low absolute values of these harmonics at their face value, especially when long feeder runs are involved. The complex analysis and harmonic method of testing outlined here seem to be essential when the higher harmonics are not negligible.

Further work will be required to bring out the relation between single tone and double tone methods of test.

12. Acknowledgments

The above work was carried out at the Standard Telecommunication Laboratories, Enfield, and permission to publish is gratefully acknowledged.

APPENDIX 1

Harmonic Generation.

Let the output for an input signal s be given by

$$V = a_1 s + a_2 s^2 + a_3 s^3 + \ldots \quad (1.1)$$

$a_1 s$ will be taken to be the recovered signal. This means that the terms of fundamental frequency produced by the higher powers of s are negligible; i.e., that $a_1 \gg a_n$. (This will certainly be so in the case of low distortion, which is the case of interest here).

Let $s = x\sqrt{2}\cos\theta$ where x is the r.m.s. amplitude.

$$\text{Now } \cos^n\theta = \frac{1}{2^{n-1}}\left[\cos n\theta + {}^nC_1 \cos\overline{n-2}\theta + {}^nC_2 \cos\overline{n-4}\theta + \ldots\right] \quad (1.2)$$

Substituting in (1) and picking out the various terms, we get (neglecting all cos θ terms except $a_1\cos\theta$)

$$V = [x\sqrt{2}a_1]\cos\theta + [2x^2a_2{}^2C_0.1/2 + (2x^2)^2a_4{}^4C_1.1/8 + (2x^2)^3 a_6{}^6C_2.1/32 + \ldots]\cos 2\theta + [(x\sqrt{2})^3a_3{}^3C_0.1/4 + (x\sqrt{2})^5a_5{}^5C_1.1/16 + (x\sqrt{2})^7a_7{}^7C_2.1/64 + \ldots]\cos 3\theta + \ldots \text{ etc.}$$

If we put $f_n(x)$ = ratio of n^{th} harmonic to fundamental, we get

$$\left.\begin{aligned} f_2(x) &= \frac{x}{\sqrt{2}a_1}\sum_1^\infty \frac{2n!}{2^{n-1}n-1!\,n+1!}a_{2n}x^{2n-2} \\ f_3(x) &= \frac{x^2}{2a_1}\sum_1^\infty \frac{2n+1!}{2^{n-1}n-1!\,n-2!}a_{2n+1}x^{2n-2} \\ f_4(x) &= \frac{x^3}{2\sqrt{2}a_1}\sum_1^\infty \frac{2n+2!}{2^{n-1}n-1!\,n+3!}a_{2n+2}x^{2n-2} \text{ etc.} \end{aligned}\right\} \quad (1.3)$$

These formulae, which are relations between amplitudes, are obviously not affected if the term $a_1x\sqrt{2}\cos\theta$ is replaced by $a_1x\sqrt{2}\cos(\theta+a)$, so that the phase of the recovered signal is of no importance here.

APPENDIX 2

Generation of Interchannel Interference.

Let us consider a multi-channel signal of N channels, N being large. If ϵ_n represents a factor which is 1 or 0 according to whether the n^{th} channel is working or not, we get the form

$$S = x\sqrt{2/\alpha N}\sum_1^N \epsilon_n\cos(npt+\theta_n) = x\sqrt{2/\alpha N}\,.\,s, \text{ say} \quad (2.1)$$

Here, $\sum_1^N \epsilon_n{}^2 = \sum_1^N \epsilon_n = \alpha N$. As explained in the text, α will be about a quarter, and the r.m.s. of S is x.

If a power series of S is under consideration, we need to handle such terms as

$$s^n = \left(\sum_1^N \epsilon_r\cos\phi_r\right)^n = \underbrace{\sum_1^N\sum_1^N\ldots\sum_1^N}_{n \text{ times}} \epsilon\cos\phi_a\cos\phi_b\ldots\cos\phi_n$$

where $\epsilon = \epsilon_a\epsilon_b\ldots\epsilon_n$ and $\phi_r = rpt + \theta_r$

If the product of cosines is replaced by sum and difference terms, it is seen that there can be all possible combinations of the form $\cos(\pm\phi_a \pm \phi_b \ldots \pm\phi_n)$. Many of these terms will be repetitions of each other, and when like terms are collected together it is found that

$$s^n = \left(\sum_1^N \epsilon_r\cos\phi_r\right)^n = 2^{1-n}\underbrace{\sum_1^N\sum_1^N\ldots\sum_1^N}_{n \text{ times}} \epsilon\left[\cos(\Sigma_n\phi_r) + {}^nC_1\cos(\Sigma_{n-1}\phi_r) + {}^nC_2\cos(\Sigma_{n-2}\phi_r) + \ldots\right] \quad (2.2)$$

The series stops at the centre term of the binomial coefficients.

$\Sigma_{n-m}\phi_r$ means $(\phi_a+\phi_b+\ldots) - (\phi_\alpha+\phi_\beta+\ldots)$ with $n-m$ positive angles and m negative angles, $a, b \ldots, \alpha, \beta \ldots$ being the suffixes which are each summed from 1 to N. The coefficients may be obtained by comparison with Equ. (1.2) to which Equ. (2.2) must reduce when either ϕ_r are all equal, or $N = 1$ (the restriction of N to large values does not yet apply).

To what extent are terms in s^n repeated in s^m when m is greater than n? Obviously, m and n must be either both even or both odd, otherwise no term can be the same. Let us take them both even, and write $2n$ and $2m$ as the indices.

To get the r^{th} term of s^{2n} from s^{2m} we need to choose $2n-r-1$ specific positive angles and $r-1$ specific negative angles from a total of $2m$ angles, the rest of the $2m$ angles cancelling out in identical pairs of positive and negative angles. The term in s^{2m} which has the requisite form, namely $2n-r+1+\frac{1}{2}(2m-2n) = m+n-r+1$ positive angles, has a coefficient ${}^{2m}C_{m-n-r+1}$. Provided N is large enough, the choice of angles can be made in ${}^{m+n-r+1}C_{2n-r+1}\times{}^{m-n+r-1}C_{r-1}$ ways, with the choice of $m-n$ self-cancelling pairs in $(m-n)!$ ways. Hence the form of the r^{th} term of s^{2n} is repeated in s^{2m} in ${}^{2m}C_{m+n-r+1}\times{}^{m+n-r+1}C_{2n-r+1}\times{}^{m-n+r-1}C_{r-1}\times(m-n)!$ different ways. This factor simplifies to ${}^{2n}C_{r-1}\,{}^{2m}C_{m-n}\,(m+n)!/2n!$ of which ${}^{2n}C_{r-1}$ is the same as the coefficient of the r^{th} term of s^{2n}. The summation over the $m-n$ self-cancelling pairs produces a further factor $\underbrace{\sum_1^N\ldots\sum_1^N}_{m-n \text{ times}}\epsilon_a{}^2\epsilon_b{}^2\ldots = (\alpha N)^{m-n}$, while from Equ (2.2) the expansions of s^{2n} and s^{2m} are seen to differ by an initial factor $2^{-(2m-2n)}$. Hence the entire s^{2n} is produced within s^{2m} with a factor $(\alpha N/4)^{m-n}\,{}^{2m}C_{m-n}\,(m+n)!/2n!$. If we use the full form S instead of s there appears an additional factor $(x\sqrt{2/\alpha N})^{2m-2n}$, giving an over-all factor $(x/\sqrt{2})^{2m-2n}\,[{}^{2m}C_{m-n}\,(m+n)!/2n!]$.

The 'multiplicity factor' in square brackets can also be obtained as follows. s^{2m} is the product of $2m$ factors s, of which any $2n$ can produce s^{2n}, while the constant term

in the remaining s^{2m-2n} will provide, with the factor s^{2n}, some multiple of s^{2n}. The choice of $2n$ factors can be made in ${}^{2m}C_{2n}$ ways, while the constant term in s^{2m-2n} is seen, from Equ. (2.2) to be ${}^{2m-2n}C_{m-n} \cdot 2^{1-2m-2n}$ times the number of ways of extracting $m-n$ self-cancelling pairs from $2m-2n$ suffixes, each running from 1 to N. This latter factor is $m-n\,!(\alpha N)^{m-n}$. Since ${}^{2m}C_{2n} \cdot {}^{2m-2n}C_{m-n} \cdot m-n\,! = {}^{2m}C_{m-n} \cdot (m+n)\,!/2n\,!$ we have the same 'multiplicity factor' as before. (In counting the number of self-cancelling pairs, such forms as $+a-a$ and $-a+a$ have been counted once only. The duplicity thereby omitted is made up for by the fact that the last term of the binomial coefficients appearing in Equ. (2.2) should carry a factor 1/2 when n is even).

Of the two derivations, the first has the advantage, however, of being 'exclusive' in the sense that it shows that no further terms in s^m occur in s^m, so that the groups of terms are now incoherent and add up power-wise.

Collecting all the terms associated with S^{2n}, we find that we have s^{2n} multiplied by

$$2^{1-2n}(x\sqrt{2/\alpha N})^{2n}\left[\sum_1^\infty a_{2n+2m-2}\,\frac{x^{2m-2}}{2^{m-1}}\,\frac{(2n+2m-2)\,!}{(m-1)\,!\,(2n+m-1)\,!}\times\frac{(2n+m-1)\,!}{2n\,!}\right] \quad . . \quad (2.3)$$

If this form is compared to the function $f_{2n}(x)$ of Equ. (1.3), they are seen to be very similar, the main difference being the occurrence in Equ. (2.3) of the factor $(2n+m-1)!/2n\,!$ multiplying the coefficient of $x^{2n+2m-2}$. Now $x^{2n+2m-2}(m+2n-1)\,!/2n\,! = (x^{2n+2m-2}/2n\,!)$

$$\int_0^\infty e^{-t}t^{m+2n-1}dt$$

$$= (1/2n\,!)\int_0^\infty e^{-t}(xt^{\frac{1}{2}})^{2n+2m-2}t^n dt$$

$$= (2x^{-2n-2}/2n\,!)\int_0^\infty e^{-z^2/x^2}\cdot(z)^{2n+2m-2}\cdot z^{2n+1}dz$$

on putting $t = z^2/x^2$.

Using this result, the expression in Equ. (2.3) can be written

$$\frac{2a_1}{2n\,!}\cdot\frac{\sqrt{2}}{x^{2n+2}}\,\frac{1}{(\alpha N)^n}\int_0^\infty e^{-z^2/x^2}f_{2n}(z)z^{2n+2}dz \quad . . \quad (2.4)$$

The extra power of z and the factor $a_1\sqrt{2}$ appear because $f_{2n}(z)$, which is a relative amplitude had been obtained by dividing by $a_1\sqrt{2}z$ in Equ. (1.3), and this factor has had to be restored in Equ. (2.4).

In order to find the relative amplitude level of the interference arising from the terms of the form S^{2n}, we need to know the amplitude of s^{2n}. Denoting by ${}^{2n}A_r$ the resultant r.m.s. amplitude of those terms in s^{2n} which fall in the r^{th} channel, and dividing Equ. (2.4) by $a_1x\sqrt{1/\alpha N}$, (the r.m.s. level of a working channel), we have the total interference level in the r^{th} channel arising from S^{2n} terms. Denoting this level by $g_{2n}(x)$ we find

$$g_{2n}(x) = \frac{2\sqrt{2\alpha}}{2n\,!}\left[\frac{{}^{2n}A_r}{\alpha^n N^{n-\frac{1}{2}}}\right]\frac{1}{x^{2n+3}}\int_0^\infty f_{2n}(z)e^{-z^2/x^2}z^{2n+2}dz \quad (2.5)$$

A similar relation is found when the power of S is odd, so that, writing n for $2n$ in Equ. (2.5), we have the general relation for all n

$$g_n(x) = \frac{2\sqrt{2\alpha}}{n\,!}\left[\frac{{}^nA_r}{\alpha^{\frac{1}{2}n}N^{\frac{1}{2}n-\frac{1}{2}}}\right]\frac{1}{x^{n+3}}\int_0^\infty f_n(z)e^{-z^2/x^2}dz \quad . . \quad (2.6)$$

There remains the calculation of ${}^nA_r$. In s^n, the term with $n-m$ positive angles and m negative angles has a coefficient ${}^nC_m$. There are $n-m\,!$ combinations of positive angles and $m\,!$ combinations of negative angles each giving the same term when the suffixes are summed. Hence, if there are α_m combinations of suffixes giving a resultant in the r^{th} channel, only $\alpha_m/(m\,!\,.\,n-m\,!)$ of them are independent and form an incoherent group. The mean-square amplitude is therefore $\frac{1}{2}\,({}^nC_m m\,!\,n-m)^2\,\alpha_m/(m\,!\,n-m\,!)$, the factor 1/2 arising as the mean square of a cosine term. This expression simplifies to $n\,!\,{}^nC_m\alpha_m/2$. The total mean square amplitude is thus $(n\,!/2)[\alpha_0 + {}^nC_1\alpha_1 + {}^nC_2\alpha_2 + \ldots]$ terminating at the centre term of the binomial series. Now α_m is the number of combinations of suffixes, $n-m$ positive and m negative, whose sum falls in the bands $+r$ and $-r$. This is the same as the number of $n-m$ positive and m negative suffixes, plus the number of m positive and $n-m$ negative suffixes whose sum falls in the band $-r$(or $+r$). This is easily seen to be the coefficient of x^{-r} in $\left(\sum_1^N x^l\right)^{n-m}\cdot\left(\sum_1^N x^{-l}\right)^m + \left(\sum_1^N x^l\right)^m\cdot\left(\sum_1^N x^{-l}\right)^{n-m}$.

The amplitude sum therefore reduces to the coefficient of x^{-r} in $\frac{1}{2}\,(n)\,!\sum_1^n {}^nC_m\left(\sum_1^N x^l\right)^{n-m}\cdot\left(\sum_1^N x^{-l}\right)^m =$

$$\frac{1}{2}\,(n)\,!\left[\sum_1^N x^l + \sum_1^N x^{-l}\right]^n$$

Summing the G.P. we get

$$\frac{1}{2}\,(n)\,!\left[\frac{1-x^{N+1}}{1-x} + \frac{1-x^{-N-1}}{1-x^{-1}}\right]^n =$$

$$\frac{1}{2}\,(n)\,!\left[\frac{1-x^{N+1}}{1-x}\,(1+x^{-N})\right]^n$$

When N is large we can replace $N+1$ by N without much error, so that we can write

$${}^nA_r{}^2 \approx (\alpha^n n\,!/2) \times \text{coefficient of } x^{-r} \text{ in } \left(\frac{x^{-N}-x^N}{1-x}\right)^n \quad . . \quad . . \quad . . \quad . . \quad (2.7)$$

The factor α^n arises from the effects of ϵ_n which have so far been neglected. α is actually the probability that any particular term is present, and with n independent terms occurring in the summations leading to ${}^nA_r{}^2$ the factor α^n accordingly appears.

Taking the square root of Equ. (2.7) and expanding both numerator and denominator by the binomial theorem we get

$${}^nA_r = \alpha^{\frac{1}{2}n}[\tfrac{1}{2}(n\,!) \times \text{coefficient of } x^{-r} \text{ in } (1-x)^{-n}(x^{-nN} - {}^nC_1x^{-(n-2)N} + {}^nC_2x^{-(n-4)N}\ldots)]^{\frac{1}{2}}$$

If we assume that r is large enough for such products as $r(r+1)$ to be replaced by r^2, we get the following fairly simple form

$${}^nA_r \approx \alpha^{\frac{1}{2}n}\left\{(n/2)[(nN-r)^{n-1} - {}^nC_1\left\{(n-2)N-r\right\}^{n-1} + {}^nC_2\left\{(n-4)N-r\right\}^{n-1}\ldots]\right\}^{\frac{1}{2}} \quad . . \quad . . \quad (2.8)$$

the terms stopping when the coefficient of N in any bracket is less than 1.

An alternative formulation is given by putting $\left(\frac{x^{-N}-x^{+N}}{1-x}\right)^n \approx \left(\frac{x^N-x^{-N}}{x^{\frac{1}{2}}-x^{-\frac{1}{2}}}\right)^n$, writing $x = e^{j\beta}$, and finding the coefficient of $e^{-jr\beta}$ by Fourier analysis. This gives $({}^nA_r)^2 = \frac{\alpha^n n\,!}{4\pi}\int_0^{2\pi} e^{jr\beta}\left(\frac{\sin N\beta}{\sin\beta/2}\right)^n d\beta$.

For N and r both large, and $\nu = r/N$ finite and less than 1, only the range near $\beta = 0$ and π is important in the integrand. Changing the variable from β to $\theta = N\beta$, the range for θ can be taken to ∞. With $\sin\beta/2 \approx \beta/2$ at the bottom of the range, this gives the asymptotic form, for large N

$$({}^nA_r)^2 \approx \frac{n\,!\,2^nN^{n-1}\alpha^n}{2\pi}\int_0^\infty \cos y\theta[\sin(\theta)/\theta]^n\,d\theta \quad (2.9)$$

Equ. (2.9) leads to the same result as Equ. (2.8) with $r = \nu N$.

It should be pointed out that although terms of the form s^n have been extracted from terms of the form s^m for m greater than n, when s^m is itself considered, no allowance has been made for the extracted terms. To this extent the approximations are of the same order as those made by Brockbank and Wass, and discussed in the text in Section 6, namely, the neglect of low-order products. But this is permissible here, since s^m with the low-order products removed is incoherent with $s^n (m > n)$, and since the interference terms of different orders are here treated as incoherent groups, the error of re-including the low-order products in s^m is at most of order $1/N$, an order of approximation which has been used elsewhere, for example in Equ. (2.9). But the inclusion of the low-order products of s^m in s^n is essential on account of their coherence. (Thus if $a \gg b$, b^2 can be neglected in the incoherent form $a^2 + b^2$, but in the coherent form $(a + b)^2 = a^2 + 2ab + b^2$, the additional term $2ab$ is not necessarily negligible. Brockbank and Wass treat all the low-order products in the first way.)

To find the 'in-phase' component of the odd harmonics, we need only those terms of ${}^nA_r$, say ${}^nB_r$, which are formed with $(n + 1)/2$ positive and $(n - 1)/2$ negative terms. This gives

$$({}^nB_r)^2 = \alpha^n \left({}^nC_{(n-1)/2} \{(n-1)/2\}! \{(n+1)/2\}! \right)^2$$
$$\alpha_{(n-1)/2} / \left(2\{(n-1)/2\}! \{(n+1)/2\}! \right) =$$
$$\alpha^n (n!/2)\ {}^nC_{(n-1)/2}\ \alpha_{(n-1)/2} \quad \ldots \quad (2.10)$$

$\alpha_{(n-1)/2}$ is the coefficient of x^r in $\left(\sum_1^N x^l \right)^{(n+1)/2} \left(\sum_1^N x^{-l} \right)^{(n-1)/2}$.

Summing the G.P., and making the same approximations as before, for large N, we get

$$\alpha_{(n-1)/2} \approx \text{coefficient of } x^r \text{ in } \left(\frac{1 - x^N}{1 - x} \right)^{(n+1)/2} \left(x^{-N} \frac{1 - x^N}{1 - x} \right)^{(n-1)/2}$$
$$= \text{coefficient of } x^r \text{ in } \left(\frac{1 - x^N}{1 - x} \right)^n x^{-N(n-1)/2}$$
$$= \text{coefficient of } x^r \text{ in } (1 - x)^{-n} \left[x^{-N(n-1)/2} - {}^nC_1 x^{-N(n-3)/2} + \ldots \right]$$
$$\simeq \frac{1}{(n-1)!} \left[(\tfrac{1}{2}N(n-1) + r)^{n-1} - {}^nC_1 (\tfrac{1}{2}N(n-3) + r)^{n-1} + \ldots \right]$$

the series stopping at the term ${}^nC_{(n-1)/2} r^{n-1}$

$$\therefore {}^nB_r \approx \alpha^{\frac{1}{2}n} \left\{ \tfrac{1}{2}n \cdot {}^nC_{\frac{1}{2}(n-1)} [(\tfrac{1}{2}N(n-1) + r)^{n-1} - {}^nC_1 (\tfrac{1}{2}N(n-3) + r)^{n-1} + \ldots \right\}^{\frac{1}{2}}$$
$$= \alpha^{\frac{1}{2}n} \left\{ \tfrac{1}{2}n \cdot {}^nC_{\frac{1}{2}(n-1)} 2^{1-n} [Nn + (2r - N)]^{n-1} - {}^nC_1 \{N(n-2) + (2r - N)\}^{n-1} + \ldots \right\}^{\frac{1}{2}}$$

Comparing with Equ. (2.8) we see that ${}^nB_r$ is obtained from ${}^nA_r$ by multiplying by $({}^nC_{(n-1)/2} 2^{1-n})^{\frac{1}{2}}$ and replacing r by $N - 2r$ (or alternatively, replacing y by $1 - 2y$). Thus instead of $h_3(y) = \frac{1}{2}(1 - y^2/3)$ in Equ. (10) of Section 5 we have

$$\bar{h}_3(y) = {}^3C_1\, 2^{-2} \cdot \tfrac{1}{2}\{1 - (1 - 2y)^2/3\} = (1 + 2y - 2y^2)/4$$

Similarly $\bar{h}_5(y) = {}^5C_2 \cdot 2^{-4}\{46 - 12(1 - 2y)^2 + (6/5)(1 - 2y)^4\}/(24)^2$
$$= 2(11 + 12y - 6y^2 - 12y^3 + 6y^4)/(24)^2 \text{ etc.}$$

When the 'in-phase' components of interference $\bar{g}_{2n+1}(x)$ have to be treated separately, the above functions $\bar{h}_{2n+1}(y)$ are used instead of $h_{2n+1}(y)$ in Equ. (10) of Section 5. The difference functions $h_{2n+1}(y) - \bar{h}_{2n+1}(y)$ must still be used to form a modified $g_{2n+1}(x)$ when the power-wise components of the interference are summed.

APPENDIX 3

Approximation to $\phi(\tau x)$.

Let $F(y,\lambda) = \int_0^\infty \cos y\theta \, [e^{\lambda \sin\theta/\theta} - 1 - \lambda \sin\theta/\theta] d\theta$.
$(\lambda = 4\pi^2 x^2)$.

At the top and bottom of the video band, $y = 1$ and 0 respectively.

We define

$$F_0 = F(0,\lambda) = \int_0^\infty [e^{\lambda \sin\theta/\theta} - 1 - \lambda \sin\theta/\theta] \, d\theta \quad (3.1)$$

$$F_1 = F(1,\lambda) = \int_0^\infty \cos\theta \, [e^{\lambda \sin\theta/\theta} - 1 - \lambda \sin\theta/\theta] \, d\theta \quad (3.2)$$

Integrating by parts, we get

$$F_0 = \theta \, [e^{\lambda \sin\theta/\theta} - 1 - \lambda \sin\theta/\theta]_0^\infty -$$
$$\lambda \int_0^\infty \theta (\cos\theta/\theta - \sin\theta/\theta^2) \, [e^{\lambda \sin\theta/\theta} - 1] d\theta =$$
$$= \lambda \int_0^\infty \cos\theta \, [e^{\lambda \sin\theta/\theta} - 1] \, d\theta +$$
$$\lambda \int_0^\infty \frac{\sin\theta}{\theta} [e^{\lambda \sin\theta/\theta} - 1] d\theta$$
$$= -\lambda \int_0^\infty \cos\theta \, [e^{\lambda \sin\theta/\theta} - 1 - \lambda \sin\theta/\theta] d\theta -$$
$$\lambda^2 \int_0^\infty \frac{\cos\theta \sin\theta}{\theta} \, d\theta +$$
$$+ \lambda \frac{\partial}{\partial \lambda} \int_0^\infty [e^{\lambda \sin\theta/\theta} - 1 - \lambda \sin\theta/\theta] d\theta$$
$$= -\lambda F_1 - \lambda^2 \frac{\pi}{4} + \lambda \frac{\partial}{\partial \lambda} F_0$$
$$\therefore F_1 = \frac{\partial F_0}{\partial \lambda} - \frac{F_0}{\lambda} - \lambda \frac{\pi}{4} = \lambda \frac{\partial}{\partial \lambda} (F_0/\lambda) - \lambda \frac{\pi}{4} \quad (3.3)$$

This relation gives F_1 in a simple way when F_0 is found. To find F_0, expand Equ. (3.1) and integrate

$$F_0 = \sum_2^\infty \frac{\lambda^n}{n!} \int_0^\infty (\sin\theta/\theta)^n \, d\theta \quad \ldots \quad \ldots \quad \ldots \quad (3.4)$$

The following values are easily obtained (e.g., Whittaker and Watson, p. 123, example 13)—

$$\int_0^\infty (\sin\theta/\theta)^2 \, d\theta = \frac{\pi}{2}; \int_0^\infty (\sin\theta/\theta)^3 d\theta =$$
$$\frac{\pi}{2} \cdot \frac{3}{4}; \int_0^\infty (\sin\theta/\theta)^4 d\theta = \frac{\pi}{2} \cdot \frac{4}{6};$$
$$\int_0^\infty (\sin\theta/\theta)^5 d\theta = \frac{\pi}{2} \cdot \frac{5}{8} \cdot \left(\frac{23}{24} \right); \int_0^\infty (\sin\theta/\theta)^6 d\theta =$$
$$\frac{\pi}{2} \cdot \frac{6}{10} \left(\frac{11}{12} \right);$$
$$\int_0^\infty (\sin\theta/\theta)^8 d\theta = \frac{\pi}{2} \cdot \frac{8}{14} \left(\frac{151}{180} \right); \text{ etc.}$$

From this we get the approximation

$$\int_0^\infty (\sin\theta/\theta)^n d\theta \approx \frac{\pi}{2} \frac{n}{2(n-1)}$$

which is exact to $n = 4$, and still nearly correct at $n = 8$. Thus a good approximation in the neighbourhood of the origin is

$$F_0 \approx \frac{\pi}{4} \sum_2^\infty \frac{\lambda^n}{n!} \frac{n}{n-1} = (\pi/4)\lambda \sum_1^\infty \lambda^n/(n \cdot n!) =$$
$$(\pi/4)\lambda \int_0^\lambda (e^\lambda - 1)/\lambda \, d\lambda$$

Jahnke and Emde define (page 2)

$$\overline{Ei}(x) = \log\gamma x + \int_0^x (e^t - 1)/t \, dt$$

Hence $F_0 \approx (\pi/4)\lambda\,[\overline{Ei}(\lambda) - \log\gamma\lambda]$ $(\log\gamma = 0.577)$ (3.5)

The probable limit of validity of Equ. (3.5) is when the eighth term of the exponential series becomes significant. which is about $\lambda = 4$. Since $\lambda = 4\tau^2x^2$ this gives $\tau x < 1$ as the upper limit.

From Equ. (3.3) $F_1 = \frac{\pi}{4}\lambda(e^\lambda - 1)/\lambda - \lambda\pi/4 =$

$$\frac{\pi}{4}(e^\lambda - 1 - \lambda) \quad .. \quad .. \quad .. \quad .. \quad (3.6)$$

To get a form usable in the range $\lambda \gg 4$, we need an asymptotic form for $\int_0^\infty (\sin\theta/\theta)^n \, d\theta$ for large n. Now when n is large, only the range near $\theta = 0$ is of value in the integrand. The forms $e^{-n\theta^2/6}(1 - n\theta^2/180)$ and $(\sin\theta/\theta)^n$ are the same up to powers of θ^4, and can be shown to give

$$\int_0^\infty (\sin\theta/\theta)^n d\theta \approx \int_0^\infty e^{-n\theta^2/6}(1 - n\theta^4/180)\, d\theta =$$

$$\frac{\pi}{2}\sqrt{\frac{6}{\pi n}}\left(1 - \frac{3n}{20}\right) \approx \frac{\pi}{2}\sqrt{\frac{6}{\pi(n + 3/10)}}.$$

This last form is very good, even for so low a value as $n = 2$. However, it cannot be used directly as the resulting series cannot be easily handled.

Now $\int_0^{\frac{\pi}{2}} (\cos\theta)^r d\theta = \frac{1}{2}\frac{\Gamma\frac{1}{2}\Gamma(r+1)/2}{\Gamma(r+2)/2}$. The form taken when r is large is easily found by using the asymptotic form for the gamma functions. With r replaced by $n - 1/5$ we get

$$\int_0^{\frac{\pi}{2}} (\cos\theta)^{n-1/5} d\theta \approx \frac{\pi}{2}\sqrt{\frac{2}{\pi(n + 3/10)}}.$$

Hence $\int_0^\infty (\sin\theta/\theta)^n d\theta \approx \sqrt{3}\int_0^{\frac{\pi}{2}} (\cos\theta)^{n-1/5} d\theta$

Using this result, it is found that

$$F_0 \approx \sqrt{3}\int_0^{\frac{\pi}{2}} [e^{\lambda\cos\theta} - 1 - \lambda\cos\theta](\cos\theta)^{-1/5} d\theta \quad (3.7)$$

The first term of the expansion of Equ. (3.6), which is the correct one, is equal to the first term of the expansion of Equ. (3.7) within 10 per cent. The succeeding terms in Equ. (3.7) rapidly approach their correct values.

Equ. (3.7) could also have been obtained, albeit in a rather superficial manner (on account of the path of integration for ϕ), by the substitution $\sin\theta/\theta = \cos\phi$ directly in Equ. (3.1), and using series expansions of θ and $\cos\theta$ in terms of ϕ.

It remains to find the asymptotic form of Equ. (3.7). For large λ only the term $e^{\lambda\cos\theta}$ is important. Expanding to the first few powers of θ, we get

$$F_0 \approx \sqrt{3}\int_0^{\frac{\pi}{2}} e^{\lambda(1-\theta^2/2+\theta^4/24)}(1 + \theta^2/10)d\theta$$

$$\approx \sqrt{3}e^\lambda \int_0^{\frac{\pi}{2}} e^{-\lambda\theta^2/2}(1 + \theta^2/10 + \lambda\theta^4/24)d\theta$$

Putting $\phi = \lambda\theta^2/2$, and taking the upper limit of ϕ to ∞, we find

$$F_0 \approx e^\lambda\sqrt{3/(2\lambda)}\int_0^\infty e^{-\phi}\phi^{-\frac{1}{2}}[1 + \phi/(5\lambda) + \phi^2/(6\lambda)]d\phi$$

$$= e^\lambda\sqrt{3\pi/(2\lambda)}\,[1 + 1/(10\lambda) + 1/(8\lambda)]$$

$$= e^\lambda\sqrt{3\pi/(2\lambda)}\,[1 + 9/(40\lambda)]$$

From Equ. (3.3) we find, for the asymptotic form of F_1

$$F_1 \approx e^\lambda\sqrt{3\pi/(2\lambda)}\,[1 - 1.275/\lambda]$$

This form is valid for values of λ greater than about 4; i.e., $\tau x > 1$.

REFERENCES

[1] Brockbank and Wass. "Non-linear Distortion in Transmitting Systems," *J. Instn elect. Engrs*, 1945, Vol. 92, Part III.

[2] L. Lewin, J. J. Muller and R. Basard. "Phase Distortion in Feeders," *Wireless Engineer*, May 1950, Vol. 27, p. 143.

[3] G. N. Watson, "A Treatise on the Theory of Bessel Functions," (2nd Edition), Cambridge University Press, 1944, p. 394, Equ. (4).

NEW BOOKS

Wireless Servicing Manual (8th edition)
By W. T. COCKING, M.I.E.E., Pp. 296 with 137 illustrations. Iliffe & Sons, Ltd., Dorset House, Stamford St., London, S.E.1. Price 12s. 6d.

Technical Instruction for Marine Radio Officers (9th Edition) (formerly Handbook of Technical Instruction for Wireless Telegraphists).
By H. M. DOWSETT, M.I.E.E., F.Inst.P. and L. E. Q. WALKER, A.R.C.S. Pp. 699 with 731 illustrations. Iliffe & Sons, Ltd., Dorset House, Stamford St., London, S.E.1. Price 60s.

The Measurement of the Time Constant of a Critically Damped Meter
By S. F. PEARCE, B.Sc., F.Inst.P. Technical Report M/T 107. Pp. 7. The British Electrical & Allied Industries Research Association, Thorncroft Manor, Dorking Rd., Leatherhead, Surrey. Price 3s.

Television
Vol. V, 1947-1948, pp. 461 + x; Vol. VI, 1949-1950, pp. 422 + x. (Reprints of articles by R.C.A. authors), R.C.A. Review, Radio Corporation of America, R.C.A Laboratories Division, Princeton, N.J., U.S.A.

Calcul Opérationnel
By ÉDOUARD LABIN. Pp. 140. (in French). Masson et Cie, 120 boulevard Saint-Germain, Paris 6e, France. Price Fr. 780.

Radio Control for Models
By G. HONNEST-REDLICH. Pp. 128. Harborough Publications, The Aerodrome, Billington Rd., Stanbridge, Nr. Leighton Buzzard, Beds. Price 8s. 6d.

Testing Radio Sets (5th Edition)
By J. H. REYNER. Pp. 215 + viii. Chapman & Hall Ltd., 37, Essex St., London, W.C.2. Price 22s. 6d.

Questions and Answers in Television Engineering
By CARTER V. ROBINOFF and MAGDALENA E. WOLBRECHT. Pp. 300 + vii. McGraw Hill Publishing Co. Ltd., Aldwych House, London, W.C.2. Price (in U.K.) 38s. 6d.

Electrical Communication (3rd Edition)
By ARTHUR L. ALBERT. Pp. 593 + ix. Chapman & Hall, 37, Essex St., London, W.C.2. Price (in U.K.) 52s.

Electric-Wave Filters (2nd Edition)
By F. SCOWEN. Pp. 188 + xi. Chapman & Hall Ltd., 37, Essex St., London, W.C.2. Price 18s.

Threshold Signals (M.I.T. Radiation Laboratory Series Vol. 24)
Edited by JAMES L. LAWSON and GEORGE E. UHLENBECK. Pp. 388 + xii. McGraw Hill Publishing Co. Ltd., Aldwych House, London, W.C.2. Price (in U.K.) 42s. 6d.